Alma Mater Studiorum – Università di Bologna

DOTTORATO DI RICERCA
in
Scienze Farmaceutiche

Ciclo XX

Settore/i scientifico disciplinari di afferenza: CHIM/08

Capillary coatings in Capillary Electrophoresis (CE) analysis of Biomolecules

Presentata da: Stefano Olmo

Coordinatore Dottorato **Relatore**

Prof. Maurizio Recanatini **Prof. Roberto Gotti**

Esame finale anno 2008

TABLE OF CONTENTS

Chapter 1 :
General remarks on capillary electrophoresis of biomolecules and capillary coatings

1. INTRODUCTION

Capillary Electrophoresis (CE) is one of the most important separation techniques in analytical chemistry, comparable to Gas Chromatography (GC) and High Performance Liquid Chromatography (HPLC). Especially CE is a very suitable technique in the separation of biomolecules (proteins, peptides, DNA) due to its unique selectivity, high resolution, high efficiency and small sample requirements as well as for the automation of the analytical procedure.

The importance of CE in protein analysis increases with the growing effort to learn more about the composition and function of proteins in living bodies. This field of studies gave birth a few years ago to a new scientific discipline called proteomics.

However, there are still many problems to solve in this approach, such as loss in efficiency, bad reproducibility of migration time and electrosmotic flow because of sample-wall interactions. Several approaches in this field have been made by using low pH, zwitterionic additives, and high ionic strength buffers. However, the chemical modification of the capillary wall is the most suitable way to solve these problems; that is, to reduce sample adsorption on the silica surface and to guarantee a controlled and reproducible electroosmosis.

Electroosmosis is one of the important factors influencing the quality and reproducibility of CE separations. The total mobility of a sample molecule is a result of the vectorial addition of the electroosmotic mobility and the electrophoretic mobility.

$$\mu_{tot} = \mu_{electrophoretic} + \mu_{electroosmotic} \qquad (1)$$

As can be seen in Eq. 1 and as is well-known from chromatography, a costant flow during analysis, from run to run and day to day is necessary to obtain reliable analytical results.

However the velocity of the electroosmotic flow is strongly dependent on many parameters, such as pH, ionic strenght, the buffer composition, and the chemical

nature of the capillary wall.

Figure 1.1 shows the dependence of the electroosmotic mobility on the pH of the buffer. The sigmoidal curve can be explained by additional dissociation of silanol groups at relatively high pH values, resulting in high electroosmotic mobilities. Some authors report a hysteresis of the electrosmotic flow when cycling from alkaline to acidic buffers and back. One reason forthis behavior might be the slow equilibration of the silica surface with the buffer medium. Additionaly, adsorption of the test solute on the capillary wall also changes the zeta (ζ) potential and, consequently, varies the electroosmotic flow.

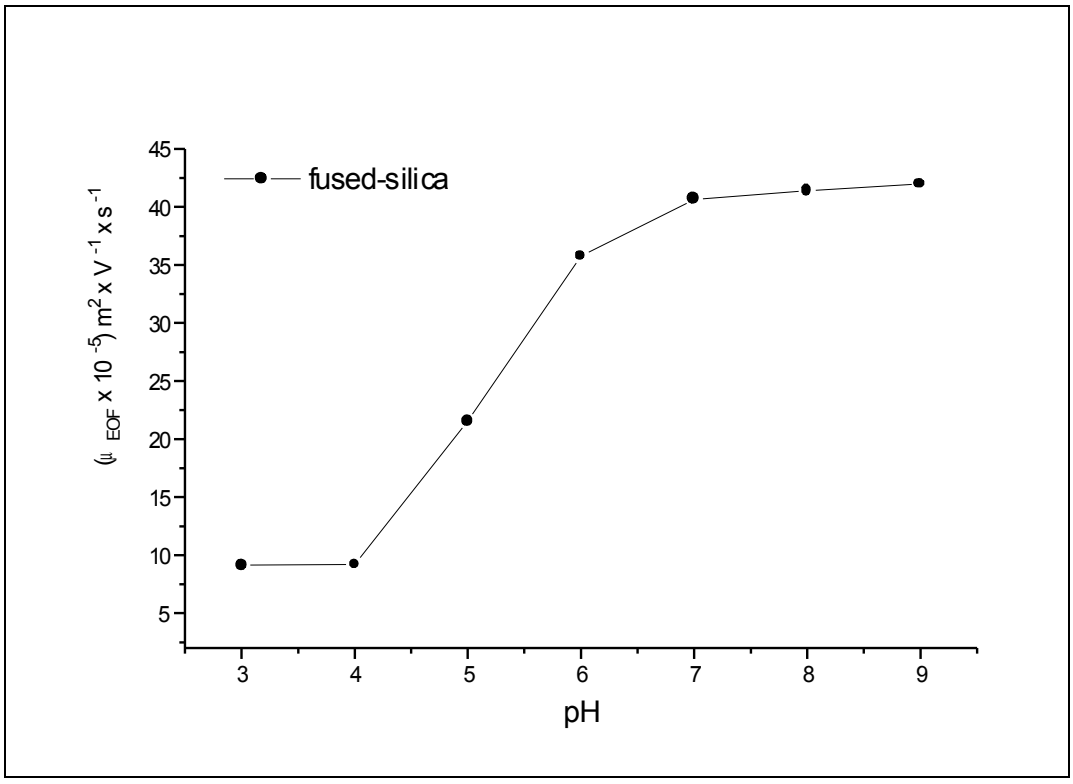

Fig 1.1. electroosmotic mobility

Chemical modification of the inner capillary are directed to cover the silanol groups and, accordingly, the electrosmotic flow will change; in fact, it should be possible to control the magnitude of EOF (till to the complete suppression) as well as its inversion.

Moreover, the use of a coating may help enhance the reproducibility of the separation

in terms of a more constant flow rate and a controlled and reversible surface interaction with solute molecules.

2. INTERACTION BETWEEN SAMPLE AND FUSED SILICA WALL

In chromatography, the main mechanism in the separation process is the interaction between the sample and the stationary phase. In CE, however, no stationary phase exists. Different solutes are separated in open tubular capillaries according to their different electrophoretic mobilities (i.e., different migration times in an electrical field).

The separation efficiency in terms of the total number of theoretical plates, N is given by Eq. 2.

$$N = \mu V/2D \qquad (2)$$

where D is the solute's diffusion coefficient and V the applied voltage. For molecules with a high relative molecular mass, the equation predicts efficiencies of several million theoretical plates. Therefore, proteins should be ideal samples fulfilling all the criteria just mentioned. However, as already reported by Jorgenson an Lukacs [1], the efficiencies for proteins observed in CE are very poor: biomolecules (especially proteins) tend to undergo serious interactions with glass and fused silica surfaces, from reversible binding to irreversible adsorption, in which the whole sample or parts of the sample sticks to the capillary wall. A nonuniform adsorption of solutes to the charged fused silica wall may lead to a nonuniform charge distribution on it, resulting in locally different electroendosmotic migration velocities, causing asimmetric zones (peaks). This strong adsorption also gives rise to poor resolution, low recovery of the separated analytes, and nonreproducible separations owing to the unpredictable changes in the magnitude of the electroosmotic flow.

The adhesive forces between the sample and the capillary wall probably are electrostatic, resulting from the negatively charged silanol groups and positively charged functionalities on the samples. Additional nonspecificic interactions, such as hydrogen bonding or van der Waals bonding may also occur.

The simplest realistic model for adsorption of proteins onto a solid nonporous surface

is depicted in Fig. 1.2 [2-4]. The first step (1) is transport of the protein to the surface. The second step (2) involves interaction and attachment of the protein to the surface. This step may involve perturbation of the protein structure. This form of the adsorbed protein may reversibly desorb from the surface. Alternatively, the adsorbed protein may relax into its steady-state conformation(s), which is irreversibly retained on the surface. If the residence time at the surface is short, the adsorption may be considered reversible. With increased residence time on the surface, proteins undergo a surface transition from “loosely” bound to “tightly” or “irreversibly” bound. For instance, freshly adsorbed myoglobin was successfully removed using 200 mM sodium dodecyl sulfate (SDS) [5]. However, if the adsorbed myoglobin was allowed to age for 24 h, an SDS regeneration of the capillary was not successful. Protein adsorption can be reversible, semi-reversible, or an irreversible process, depending on the system. Steps 2 and 3 in Fig. 1.2 are primarily controlled by direct forces (e.g., coulombic and hydration forces) between the protein and the surface, but also include interactions with water, other adsorbed proteins and buffer components in the interfacial region.

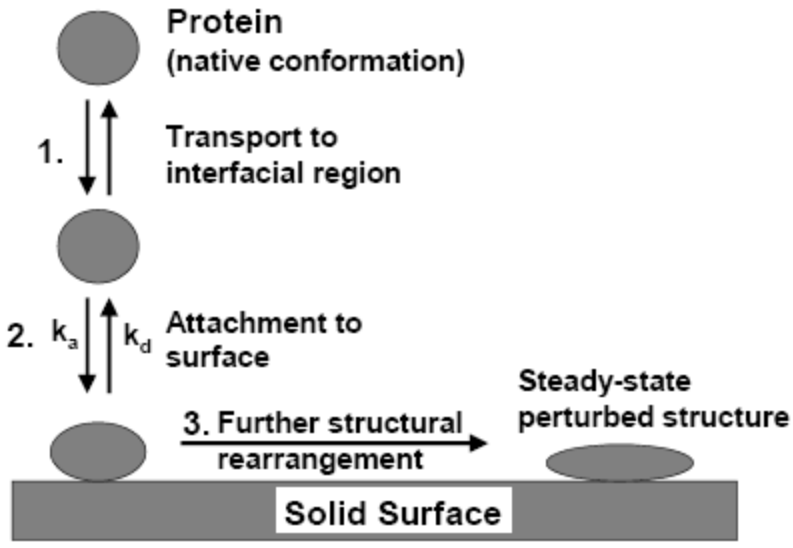

Fig. 1.2. Simple model of protein adsorption.

Norde and Haynes contend that no type of molecular interaction is unimportant in the adsorption process [2]. However, the main driving forces for protein adsorption are electrostatic and hydrophobic interactions, as well as structural changes in the protein. Electrostatic interactions depend on the surface charge and the protein charge, both of which are dependent on pH and electrolyte composition. Usually the hydrophilic amino acids of a protein are located on the periphery, because they are the ones that interact with the aqueous environment. However, if the residues are present in the interior of the protein they occur as ion-pairs. Hydration or ionization of the ionic groups buried within the low-dielectric interior of the protein in the non-ionized form, may play a significant role in protein unfolding [6].

Positively charged proteins with p*I* values well above the buffer pH (e.g., lysozyme, cytochrome *c*, ribonuclease A, and α-chymotrypsinogen A) are quantitatively adsorbed onto the fused silica. Proteins with p*I* near the buffer pH of 7.0 such as myoglobin and conalbumin show only partial adsorption, while proteins with p*I* well below pH 7.0 show increasing recovery as a result of the coulombic repulsion between the anionic protein and the silica surface. Therefore, as the net charge of these proteins becomes increasingly negative, there is less adsorption on the capillary surface. Protein adsorption is not solely explained by the net charge or charge density of the protein. Rather, charge localization on the protein plays an important role in protein adsorbant electrostatic interactions [7,8]. Protein configurations, in which numerous positive protein charges are close to adsorbant charge, produce the most favorable binding [7]. Consequently, conformational flexibility of the protein plays a role in the strength of the electrostatic interactions. However, subtle effects such as the stronger binding of arginine than lysine residues makes it clear that other effects such as hydration must be included to fully explain protein adsorption.

Hydrophobic dehydration results from bonding of the protein's hydrophobic patches to hydrophobic surfaces. Hydrophobic dehydration is relatively unimportant for hydrophilic surfaces and/or hard hydrophilic proteins. Hydrophobic dehydration was recognized by Kauzmann as a driving force in protein folding [9]. Dehydration of the

nonpolar residues in an aqueous environment results in an increase in the entropy of the water molecules in the vicinity of these residues. As a result, the hydrophobic residues aggregate. The degree to which hydrophobic dehydration imparts stabilization to the protein is determined by the hydrophobicity of the amino acids. The secondary structure of the protein is destabilized if there is a reduction in these forces. In terms of protein adsorption, an increase in the hydrophobicity of the surface leads to an increase in adsorbed protein [3,6]. With respect to properties of proteins, the stability of the structure (hard or soft), size, charge, amino acid composition, and steric conformation may affect the adsorbed amount [10]. As alluded to above, the stability of the protein structure is of particular importance. Globular proteins such as lysozyme, α-chymotrypsinogen, ribonuclease, and β-lactoglobulin have high internal stability, and so are often referred to as "hard" or rigid proteins [3,11,12]. Only small amounts of these hard proteins adsorb on hydrophilic surfaces unless there is electrostatic attraction, which leads to a structural change upon adsorption onto the surface. Such globular proteins have been the most common model proteins for studies of CE coatings.

To accurately reflect the efficacy of a capillary coating for preventing protein adsorption it is necessary to have measures of both the reversible and irreversible adsorption depicted in Fig. 1.2.

Measures of reversible adsorption include:

(a) peak efficiency in terms of plate height or plates/m;

(b) protein mobility;

Measures of irreversible adsorption include:

(c) change in EOF mobility;

The considered points will be discussed below:

a) Peak efficiency

The most common mean of monitoring the effectiveness of a capillary coating is to measure the peak efficiency (N). Ideally peak broadening in CE is governed solely by

longitudinal diffusion.

Schure and Lenhoff [13] investigated the effect of mass transport to the capillary surface (i.e., step 1 in Fig. 1.2) on broadening under linear isotherm conditions (i.e., the adsorption/desorption equilibrium of step 2 in Fig. 1.2 is facile and the amount adsorbed on the surface is small relative to the adsorption capacity of the surface). One conclusion from their work is that in the absence of Joule heating there is little advantage to using narrower capillaries for large molecules such as proteins. Was then experimentally observed that the plate height increases with increasing migration velocities of model proteins [14].

The loss in efficiency due to the slow radial diffusion and slow adsorption/desorption kinetics is an indicator of reversible protein adsorption (Fig.1.2).

b) Migration time

Clearly, changes in EOF velocity would alter the migration time of an analyte. In addition, reversible adsorption onto the capillary wall retards the migration of the protein [15]. This was recently illustrated by Fang et al. who used a two-dimensional CE simulation model [16] to generate a quantitative description of adsorption in CE (Fig. 1.3). In the absence of any adsorption onto the wall, a Gaussian peak at 97.8 s is observed. Injection of a sufficiently small amount of analyte (e.g., 0.005 mol m^{-3}) such that the amount injected is small compared to the number of adsorption sites results in a broader Gaussian peak shifted to a longer migration time (128.9 min). This broadening is due to slow adsorption/desorption under linear isotherm conditions. A second observation within Fig. 1.3 is that as the concentration of protein injected increases (0.01→10 mol m^{-3}) an increasing fraction of the adsorption sites are occupied. This results in a shift in the migration time, and an increase in peak asymmetry and efficiency loss. Thus, both losses in efficiency and changes in the migration time of a protein peak are indicators of reversible adsorption. Such changes in migration time are usually reflected by an increase in the relative standard deviation (RSD) of migration time for successive injections (run-to run).

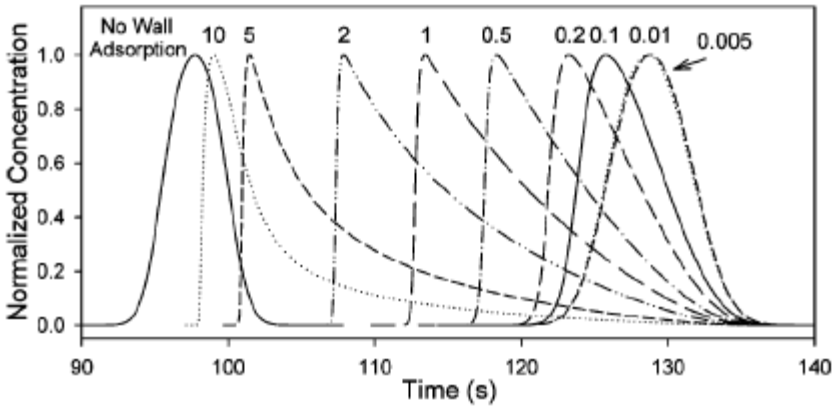

Fig. 1.3. Simulated peak profiles for various injected analyte concentrations onto a capillary possessing an adsorption capacity of 4 x 10^{-6} mol m^{-2} of binding sites [Lucy]

c) EOF

Adsorption of protein onto the capillary surface alters the electroosmotic flow velocity by altering the zeta potential at the capillary inlet [17]. Thus, the stability of the EOF during a series of protein injections can serve as a simple and effective means of monitoring protein adsorption. Graf et al. monitored the EOF during injections of the model proteins cytochrome *c*, myoglobin, ovalbumin, and β-lactoglobulin onto a bare silica capillary [5]. Fig. 1.4 illustrates the EOF behavior observed during a series of injections of 0.29 mg/mL cytochrome *c*. Initially a series of 30 injections of just the EOF marker were performed (e.g., ▲ pH 10.5 pre) to establish the reproducibility of the EOF in the absence of protein adsorption. Next 30 injections of cytochrome *c* and the EOF marker were performed (* pH 10.5 Cyto). The EOF change clearly illustrates the adsorption. Finally, a series of 15-30 injections of EOF marker was performed (■ pH 10.5 post), which show that the adsorbed protein continues to alter the EOF. Thus, EOF reproducibility can be used as a simple measure of whether irreversible adsorption is occurring.

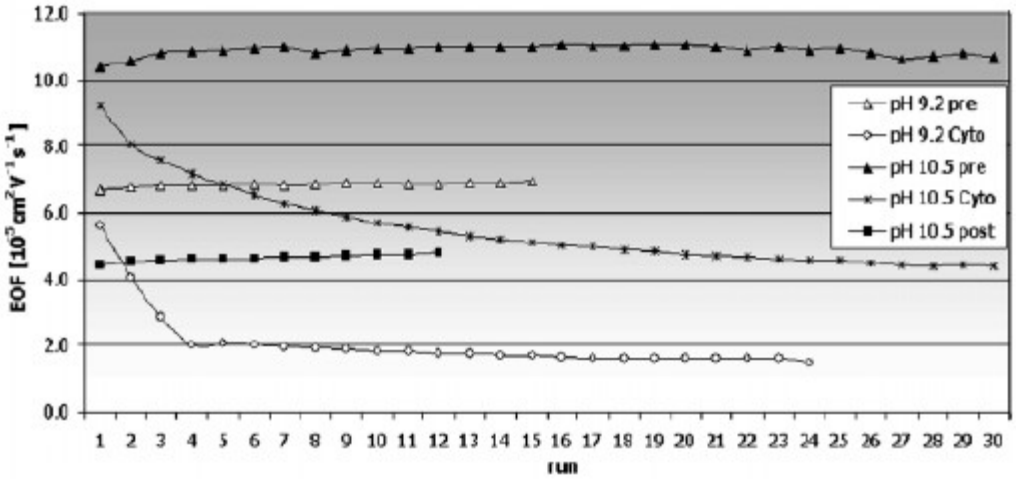

Fig. 1.4. EOF mobility observed over 30 successive injections of cytochrome c (p*I* = 9.59) onto a bare silica capillary.

By modifying the wall chemically with a neutral coating, ion-exchange interactions with dissociated silanol groups are reduced. Moreover, steric hindrance can also prevent the solvents from being adsorbed. In this way, any interactions, other than electrostatic, are suppressed.

3. CAPILLARY COATINGS

Several attempts have been made to alleviate the problem of solute-wall interactions. These approaches can be classified into two main categories: one category comprises all the methods that allowed the use of untreated fused silica capillaries by providing certain electrophoretic conditions that minimize electrostatic interactions between the analytes and the capillary wall, and another category combines all the approaches dealing with the permanent modification of the capillary wall to produce an inert nonadsorptive surface.

Untreated fused silica capillaries with their ionizable surface silanols, function as cation exchangers toward positively charged species. Solute-wall interactions may not be problematic for the separations of small and positively charged species by CZE, however, owing to the polyionic nature of large biomolecules, multipoint attachment of the analyte to the charged surface may cause band broadening or no elution of the analytes. In fact, capacity factors of only 0.05 can result in a 20-fold reduction in the separation efficiency of the proteins [16]. Therefore, the separation of proteins with untreated fused silica are possible only under electrophoretic conditions whereby electrostatic interactions can be minimized. The strategies used so far to achieve this goal are (a) inducing coulombic repulsion between the analyte and the capillary wall by raising the pH of the buffer solution above the isoelectric points (pI) of the solutes; (b) operating with buffers of low pH, whereby the surface silanols are not ionized; (c) using relatively high salt concentration in the running buffer so that the counterions would compete with the solute for the available binding sites in a manner similar to ion-exchange chromatography; and (d) the inclusion of various additives in the running electrolyte that can either associate with the solute or the silica surface, thereby reducing the extent of solute-wall interaction.

Although untreated fused silica capillaries can be used in the analysis of proteins under certain conditions, various limitations do exist, such as narrow pH range, high conductivity, low detection sensitivity, and the ability to analyze only one class of proteins. All together this limits the range of applicability of narrow-bore silica

capillaries and does not provide a universal solution for the solute-wall interaction problem especially for large peptides and proteins.

Coating the capillary is the suitable way to prevent this drawback and, as widely reviewed, many are the approaches proposed to perform the coverages including dynamic deactivation of the silica surface and permanent modification of the inner capillary wall by covalent or noncovalent layers. Among the latter, charged polymers physically adsorbed onto the capillary wall have shown good performances in protein analysis and recently, very stable coatings have been obtained by the alternative adsorption of polymers with opposite charge in order to obtain multiple layers. Mazzeo and Krull [18] identified the four features that an ideal coating should exhibit for the efficient analysis of proteins: (1) separation efficiency (in theory this should approach 1-2 million plates/m); (2) protein recovery (this should approach 100%); (3) reproducibility of migration time from run to run and day to day; and (4)
retention of the electroosmotic flow (EOF) so that cationic and anionic proteins can be separated in the same run. To these Lucy et al. [19] added that the coating should also ideally be: (5) easy to generate; (6) inexpensive; (7) applicable over a wide range of buffer conditions; and (8) should not interfere with detection (i.e., should be compatible with both optical and mass spectral detection).

3.1. Dynamic Coatings

Dynamic wall coating is an attractive coating method because it overcomes difficulties in carrying out reproducible, homogeneous chemical derivatization reactions in the capillary lumen. Dynamic coatings do not eliminate EOF completely but can be easily prepared by rinsing the capillary with a solution of a polymer, detergent, or multivalent ions; a little amount of the coating material is usually added to the separation medium to keep the coating on the silica wall surface. Improvement of CE separation in dynamically coated capillaries may be sufficient for the analysis of simple protein mixtures without necessity to use more sophisticated static coatings. Adsorption of model proteins (cytochrome *c*, myoglobin, ovalbumin, and β-

lactoglobulin) on fused-silica capillary was investigated during CZE. A pH dependence of adsorption was observed in bare fused-silica capillaries with a clear correlation to the respective p*I*. For myoglobin and ovalbumin, negligible adsorption was found above their p*I*, whereas below the p*I,* a strong cationic adsorption occurred. Cytochrome *c* and β-lactoglobulin already showed distinct adsorption above their p*I*. None of the proteins exhibited any significant adsorption more than one pH unit above the p*I*. For linear polyacrylamide coated capillaries, a decreased pH dependent adsorption was observed but it was not completely eliminated. The lifetime of a dynamic-coated capillaries can be extended by using an occasional, simple regenerating process with a solution of the coating agent. Regeneration of the capillaries by rinsing with buffers containing 200 mM SDS was also investigated. This method was successful for freshly adsorbed myoglobin; after storage of 24 h, a satisfactory regeneration was impossible [5].

Many types of polymeric and small molecular mass buffer additives are used as dynamic coatings. As Righetti *et al.* [20] reviewed, among all the possible additives, perhaps the class which has received the greatest attention is that of the amino modifiers. This class comprises a vast numbers of compounds, starting from monoamines, such as triethylamine and propylamine [21,22], morpholine [23] *N,N*-diethylethanolamine, triethanolamine [24], as well as the quaternary base tetramethylamonium chloride [25]. Among the diamines: 1,3 diaminopropane [26] and ethylenediamine [27]. Among the polyamines, we can list chitosan [28] and polyethyleneimine (PEI) [29]. Systematic studies by Verzola et al [30,31] showed that:

(i) Monoamines (e.g., glucosamine and galactosamine) are very poor at preventing protein interactions with the silica wall.

(ii) Diamines (e.g., cadaverine, putrescine) are slightly better, but ca. 120–150 mM is necessary to achieve 90% interaction inhibition [30]

(iii) Triamines (spermidine, diethylenetriamine) offer a much improved binding inhibition, and can be effective at 40 mM [32];

(iv) Polyamines, such as spermine and tetraethylenepentamine, offer 90% binding inhibition at levels of ca. 1–2 mM [30].

The drawback of these additives, though, is that they loose efficiency when working at alkaline pH ranges, due to the deprotonation of the various amino groups. Also anionic and zwitterionic polymers have been described as potential additives inhibiting protein interaction with the silica wall, but most of all neutral polymers are used as coating agents added to the buffer. Neutral polymers could be divided into two classes: (i) Neutral, hydrophilic polymers such as: cellulose and dextran [33-36]; poly(vinyl alcohol) [37,38] and polyethylene oxide (PEO) [39]; (ii) neutral hydrophobic polymers such as cellulose acetate.

In 1992 Lindner *et al*. [40] showed the effectiveness of a 0.03 % solution of Hydroxypropylmethyl cellulose (HPMC) in an aqueous acidic BGE in preventing the adsorption of histones to the capillary in CE. In particular, the separation of acetylated and non-acetylated forms of H4 and H3 histones, which are among the most basic naturally occurring proteins known (p*I* 11 – 12), was obtained. Similar conditions allowed also the separation of phosphorilated H1 histone variants [41]. The reliability of the proposed CE system was also proved by recent applications related to the evaluation of histone modifications in cancer cells [42, 43].

A dynamic coating has been prepared by adding a cationic polysaccharide amylopectin to BGE. Capillaries with this dynamic coating generated reversed EOF, stable in the pH range 4–8. The run-to-run and batch-to batch reproducibilities were 0.5 and 2.4%, respectively. Chymotrypsinogen A migrated with separation efficiency of 560 000 plates/m [44]. Copolymers containing various amounts of ethylpyrrolidone methacrylate and dimethyl methacrylate have been prepared and tested for suppressing EOF in bare capillaries. Changing the relative content of the monomers in the copolymer, enabled the positive charge of the copolymer to be tailored. Selected copolymers provided reproducible reversed EOF and reduced adsorption of basic proteins on the capillary wall [45].

Various surfactants have been used to reduce EOF and protein adsorption on the wall,

including the cationic detergent didodecyldimethylammonium bromide [46], neutral surfactant Brij 35 modifying hydrophobic channels in a poly(dimethyl siloxane) (PDMS) microchip [47], zwitterionic sulfobetains [48,49], zwitterionic 1,2-dilauryloyl*sn*-phosphatidylcholine [50,51], and 1,4-didecyl-1,4-diazoniabicyclo[2,2,2]octane dibromide [52]. The phospholipid coating was more efficient in reducing EOF, if it was stabilized by the addition of divalent cations (Ca^{2+}, Mg^{2+}, Zn^{2+}) or by working in the gel-state region of the phospholipid [53]. Similarly zwitterionic surfactants 1-palmitoyl-2-oleyol-*sn*-glycero-3-phosphocholine [54] and 1,2-dioleyol-*sn*-glycero-3-phosphocholine [55] were also used as a dynamic coating, the latter after a free-radical-initiated polymerization. A dynamic coating based on mixed cationic/anionic surfactants (CTAB and SDS) has also been prepared [56]. Various synthetic and natural polymers that not only affect electrokinetic potential of the wall but also increase viscosity at the capillary wall have been also used as a dynamic coating. Quarternary ammonium-substituted agarose [57], poly(*N*-hydroxyethyl acrylamide) [58], cationic polymer polyE-323 [59], Polybrene [60] , hyperbranched poly(amino ester)s [61,62], copolymer of 2-ethyl-(2-pyrrolidine) methacrylate and *N*,*N*-dimethylacrylamide [63,64], PVP and poly(methyl methacrylate) [65], poly(aminophenyl boronate) [66], and a commercially available polymer of undisclosed composition EOTrol™ [67] were used recently as dynamic coatings in CE.

Self-coating sieving matriches can also be used as an effective means of establishing the dynamic coating on the capillary wall. In this case, the capillary is filled with a polymer solution that partly adsorbs to the capillary surface, forming a dynamic coating and, simultaneously a three-dimensional sieving matrix for separation of various biomolecules in CE.

3.2. Static Coatings

An attractive way to avoid the adsorption to the capillary wall is to develop a static coating, in which the coating material could be either physically adsorbed or

covalently bonded to the silica surface.

The most commonly used materials in developing these kind of coatings are usually charged or neutral polymers.

3.2.1. Phisically adsorbed coatings

The adsorption of charged polymers usually introduce positive or negative charges on the surface, thus changing the direction and/or the strength of the EOF, as well as the analyte-wall interaction in the separation capillary. This method is usually used to solve a specific separation problem, *i.e.*, fast separation of positively charged analytes. Reversed EOF can be achieved by coating capillaries with strong cationic polymers such as polyamines, poly(dimethyldiallylammonium chloride) (PDMAC) [68], polybrene (PB) [69] and polyarginine (PA) [70].

Polycationic polymers are electrostatically attracted to the negatively charged surface of fused silica capillaries. The preparation of an adsorbed cationic polymer coating is based on two steps [71]. In the first step, the silanols are activated, typically with a NaOH rinse. Next in the second step, the capillary is flushed with a solution of a polycationic polymer, which adheres strongly to the negatively charged capillary. Commonly the polymer solution is allowed to sit in the capillary for some time to ensure full coverage of the surface. A few methods increase the stability of the coating by cross-linking the adsorbed polymer. The positively charged surface that results generates a reversed (anodic) EOF.

Cationic capillary coatings effectively separate positively charged proteins, peptides, and drug samples.

In particular, the analysis of anionic small molecules can be obtained under co-electrosmotic conditions, thus resulting in shorter analysis times compared to the separation under counter-EOF conditions.

Use of high molecular weight PEI (600 000 to 1 000 000) enabled coatings to be formed simply by flushing the capillary with polymer solution for 10 min and then allowing the capillary to stand for 1 h [72]. The PEI coating was stable over the pH range 3-11, although the magnitude of the anodic EOF gradually decreased at pH >6.

Efficiencies for protein separations were moderate [72,73], and were dependent on the separation buffer used [74]. The reproducibility of migration times was 0.5-1.5% (n=6) for run-to-run and 1.9-2.8 % (n=18) for capillary-to-capillary [72]. The EOF reproducibility was not noticeably changed by addition of a small quantity of PEI in the BGE, although selectivity changes in the protein and peptide separations were observed [73].

Finally it was noted that the EOF of PEI coated capillaries was strongly dependent on the type of anion in the BGE [72,73], and that the direction of the EOF could even be altered if multiply charged anions are present [74]. These EOF changes reflect the adsorption of these anions onto the positively charged surface.

A stable wall modification was accomplished by creating successive multiple ionic polymer layers (SMIL) [75]. In this approach an anionic polymer (*i.e.,* dextran sulfate) was tightly fixed to the capillary wall by a cationic polymer (*i.e.,* polybrene) electrostatically attached to the uncoated fused silica capillary (Fig.1.5). Reproducibility of this coating process was excellent, and the capillary demonstrated an acceptable lifetime. Recenlty a three-layer coating (A+/B-/C+) was prepared by a successive multiple ionic polymer layer technique. It comprised high-molecular-mass polyethyleneimine (PEI) as the bottom layer and a cationic protein as the upper layer [76].

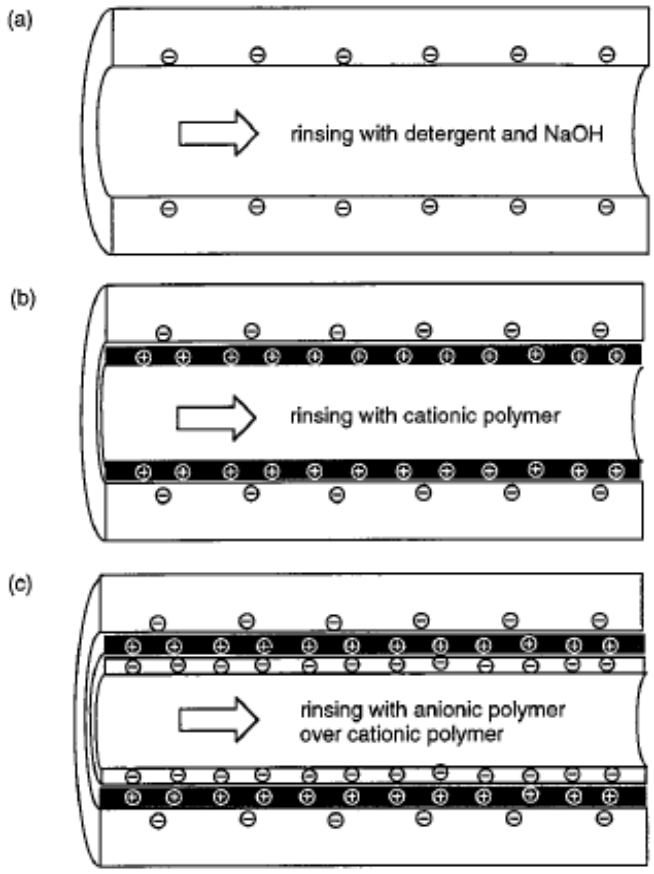

Fig. 1.5. Coating procedure for polycationic polymer coatings (steps a-b) and Successive Multiple Ionic-polymer Layer (SMIL) coatings (steps a-c).

A new polymer poly-LA 313 has been synthesized and applied as a physically adsorbed polyamine coating for CE. The coating was durable in the pH range 2–10 and in the presence of organic modifiers [77].

The goal of introducing neutral polymers to the capillary surface is usually to reduce or eliminate EOF as well as analyte-capillary surface interaction. The hydrophilicity of the coating polymer is very important: increasing the hydrophilicity will reduce sample-wall interaction in biopolymer separations, however it will reduce the stability of the adsorbed coating.

Neutral hydrophilic polymers interact with the silica surface primarily through hydrogen bonds formed between functionalities within the polymer and the protonated silanols on the surface. Thus, pretreatment of the silica surface to generate

protonated silanols is an important factor in maximizing the stability of adsorbed neutral polymer coatings.

Several cellulose derivatives are coating agents that effectively mask surface silanols and suppres EOF.

Methyl cellulose was one of the first coatings used in CE. More recently cellulose acetate (CA) coatings were prepared by rinsing a capillary with 1% w/v CA dissolved in acetone and drying under helium. CA coated capillaries possess a suppressed EOF and are stable over the pH range 2-7.5. Above pH 7.5 the performance declined. The RSD of the migration times of basic proteins was 0.2-0.4% (n=5). High efficiencies were achieved for basic proteins, but only moderate efficiencies for acidic proteins. The CA coating stability, examined by monitoring efficiencies, was stable after 75 successive runs. Fully hydrolyzing the triester yielded cellulose triacetate (CTA). A capillary coated with 1% w/v CTA yield high efficiencies for basic proteins [78].

Hydroxypropylmethylcellulose (HPMC) and hydroxyethylcellulose (HEC) can be used as a coating and sieving matrix for DNA restriction fragments. Cellulose-based adsorbed coatings can easily be washed off the capillary wall because of their hydrophilicity, that's why these coatings need regenerating processes.

To immobilize the cellulose coating on the wall, thermal treatment at 140°C can promote a chemical reaction between the hydroxyalkyl-substituted cellulose and the fused-silica inner capillary wall [79]. The resulting immobilized cellulose-coated columns are stable between pH 3 and 10.

Cellulose acetate, cellulose triacetate and cross-linked hydroxypropylcellulose (HPC) are polymers with good film-forming properties. Using these features, the polymers were first dynamically coated onto the silica surface and then phisically adhered (“skin coating”) by helium purging [78]. Unfortunately, the stability of this skin coating is very limited, so it can only be used at pH < 7.5.

Capillaries coated with HPC cross-linked with paraformaldehyde yielded migration time RSDs of 0.4-0.5% (n=10) and high efficiencies for basic model proteins. Recently, HPC coated capillaries have been used for the separation of monoclonal

antibodies [80].

Poly(vinyl alcohol) (PVA) binds more strong to the silica surfaces than HEC, so columns coated with this compound have improved stability. These kind of coated capillaries offer good separations of biopolymers. Permanent PVA coating can be readily achieved by thermal immobilization. Thermal treatment (140°C under N_2 for several hours) of a thin film of PVA (MW 50 000, 99+% hydrolyzed) yields a pseudocrystalline structure with reduced water solubility and swelling properties [37]. High separation efficiencies were obtained at pH 3.0 and moderate-to-high efficiencies for basic proteins at pH 5.5, but lower efficiencies were observed at pH 10. The thermally treated PVA strongly suppressed the EOF at pH 4-10. At pH 3.0 the RSD of migration times for five basic proteins was 1.3-2.1% over 60 injections, with no changes in peak symmetry or width. At pH 8.5 the performance of the PVA coated capillary decreased abruptly after 40 runs.

This coating has been used for the separation of protein glycoforms [37] and in field amplified sample stacking of basic proteins [81].

There are other neutral polymers used as physically adsorbed coating for separation of biomolecules, such as poly(ethylene glycol) (PEG), poly(ethylene oxide) (PEO) used either as sieving matrix [82] or as coating agent [39].

Madabhushi [83] introduced a low-viscosity polymer solution, poly(dimethyl acrylamide) (PDMA) as a self-coating sieving matrix for DNA sequencing. Although PDMA as excellent adsorptive properties, is rather hydrophobic, which is undesirable for protein and DNA separations. To combine adsorbing properties with hydrophilicity, a co-polymer of dimethyl acrylamide and allyl-glycidyl ether: poly(dimethylacrylamide-*co*-allyl glycidyl ether) (EPPDMA) was introduced [84]. These adsorbed coating capillaries offer excellent separation in DNA fragments analysis [84]. The EPPDMA capillaries showed excellent stability and no treatment was necessary for over 200 sequencing runs (300 h). After that regeneration was achieved in less than 1h simply rinsing the column with an alkaline solution followed by the coating polymer solution.

3.2.2. Covalently bonded (or Permanent) coatings

A permanent wall coating is an attractive way to eliminate EOF and wall-analyte interaction in the separation capillary. Physically adsorbed coated capillaries require occasional regeneration, and dynamic coating is obtained by adding the coating material to the running buffer, so the high power of hyphenated CE-MS cannot be exploited. The use of uncoated capillaries with self-coating matrices is compelling, but the capillary performance deteriorates during repetitive runs and extensive rinsing is required between runs.

Consequently there is a strong driving force to prepare hydrolitically stable, reproducible, covalently bonded capillaries for various separation purposes. Preparation of a permanent wall coating typically consist of three steps: i) capillary pretreatment, ii) introduction of double bonds to the capillary wall, and iii) binding of a polymer to this intermediate layer.

i) To achieve the best coating results, the capillary surface must be cleaned and activated by etching and/or leaching prior the coating process. The effect of each capillary preparation step (etching, leaching, dehydration, silylation, and coating) on the final performance of the column has been studied extensively. Optimal coating reproducibility requires column etching with sodium hydroxide followed by leaching with hydrochloric acid. To improve the yield of the silylation reaction, all water has to be removed from the surface: 160°C overnight dehydration allow the best result [85].

ii) Attaching a polymer coating to the capillary wall can be done easily using a reactive bifunctional silane such as γ-methacryloxy propyl trimethoxy silane described by Hjertèn [86]. The surface silanols react with the silane group of the reagent, then the other functional group is used to attach the coating agent to the capillary.

The main disadvantage of using silanes to deactivate the silica surface is that the resulting siloxane bond offer unsatisfactory hydrolytic stability at alkaline pH. To improve the stability of the final coating Cobb and co-workers [87] replaced the Si-

O-Si bonds with Si-C bonds in a procedure using Grignard chemistry.

Pesek *et al.* [88] introduced another method of forming an hydrolytically stable intermediate layer based on hydride-silica chemistry. The method uses catalytic hydrosilylation of terminal olefins on a SiH-containing substrate.

Another method uses a sol-gel process to prepare a stable, homogeneous sublayer with high density of polymerizable olefinic groups. Formation of this sublayer was independent of the initial surface properties of the fused-silica capillary, and the process is robust and easy to use. The resulting layer is very stable: at pH 10, the EOF remains constant on a low level over a long period of time [89].

iii) Finally, by covalent bonding, small molecules and polymers either polymerized in situ or preformed, and then subsequently cross-linked to increase surface coverage, are attached to the wall.

The development of a permanent coating allows to efficient column for protein separations, minimized lot variation and promoted reproducibility during consecutive runs; but the complexity and multiplicity of steps required in the preparation of the former often lead to poor coating-to-coating reproducibility.

Many are the compounds used to develop these kinds of coatings, most of all neutral and and charged hydrophilic polymers.

Between neutral polymers, poly(acrylamide) has been used in many wall coatings [86,87]. An extensive study evaluated the effect of polymerization on properties of the final acrylamide coated capillary [90]. Leftover unreacted acrylamide monomer in the wall coating can substantially increase the background absorbance (even at 254 nm) and leave potentially harmful reacting species in the background electrolyte. Consequently, a chemical scavenging method using cysteine was proposed to remove such material [91]. Poly(acrylamide) is a superb capillary coating, but is rather unstable at alkaline pH. Tremendous effort has, therefore, been dedicated to studying and improving its hydrolytic stability. One way of improving this stability is to cross-link the linear polymer chains. When a cross-linked polyacrylamide (acrylamide + bisacrylamide) coating was used instead of linear chains, the lifetime of the coating

improved significantly. Efficient protein separations were achieved by using cross-linked sub- and toplayers [92]. First poly(vynimethyl siloxane-diol) was attached and cross-linked to the surface of a fused-silica column, then polyacrylamide was grafted to the top of this polymeric sublayer. Finally the linear poly(acrylamide) (LPA) toplayer was cross-linked with formaldehyde.

The strongly hydrophilic and neutral polymer, poly(vinyl alcohol) (PVA), can be used either as a dynamic coating (buffer additive) as previously mentioned, or as a water-insoluble covalent coating on fused-silica surface, PVA can be covalently attached by pretreating the capillary with a glutaraldehyde cross-linking agent followed by a solution of PVA. Migration time reproducibilities of ≤1.3% and high efficiencies were observed for basic proteins over 1150 repetitive injections [93].

Many polisaccharides such as dextran and cellulose derivatives such as HPMC can be used to develop permanent coatings.

As previously shown HPMC was successfully used as buffer additive in the analysis of histones; in order to profit of this benefical effect of HPMC on histone separations by CE-MS applications, Aguilar *et al*. [94] proposed a method in which HPMC was used as a permanent coating onto the capillary surface. The adopted coating procedure was according to that previously optimised by Liao *et al*. [35] and consisted in the functionalisation of the silanol groups of the inner capillary wall with a sililating reagent bearing an epoxy group; the stable coating was then created by coupling covalently the epoxy moiety with the hydroxyl groups of the polymer.

Introduction of positive surface charges can significantly reduce interaction with basic proteins, but irreversible adsorption of acidic proteins may occur. Binding weak cationic polymers to the surface creates a pH-dipendent positive charge on the surface. The pH dependence of EOF in fused silica capillaries can complicate CE method development. Strong cationic polymers such as a reactive polyamide resin [95], poly(vinilamine) [96] and PEI coating [97] can be used to develop permanent positive coatings for separations of basic analytes.

References

[1] J.Jorgenson, K.Lukacs, Science 222 (1983) 236

[2] W. Norde, C.A. Haynes, in Proteins at Interfaces II: Fundamentals and Applications, American Chemical Society, Washington, DC, 1995, p. 26.

[3] W. Norde, in A. Baskin, W. Norde (Editors), Physical Chemistry of Biological Interfaces, Marcel Dekker, New York, 2000, p. 115.

[4] M. Malmsten, J. Colloid Interf. Sci. 207 (1998) 186.

[5] M. Graf, R.G. Garcia, H. Watzig, Electrophoresis 26 (2005) 2409.

[6] W. Norde, in Surfactant Science Series (Biopolymers at Interfaces), Marcel Dekker, New York, 2003, p. 21.

[7] Y. Yao, A.M. Lenhoff, Anal. Chem. 76 (2004) 6743.

[8] Y. Yao, A.M. Lenhoff, Anal. Chem. 77 (2005) 2157.

[9] W. Kauzmann, Adv. Protein Chem. 14 (1959) 1.

[10] K. Nakanishi, T. Sakiyama, K. Imamura, J. Biosci. Bioeng. 91 (2001) 233.

[11] P. Le Duc, Y. Wang, in S.A. Guelcher, J.O. Hollinger (Editors), Introduction to Biomaterials, CRC Press, Boca Raton, FL, 2006, p. 47.

[12] A.D. Bhaduri, K.P., J. Disper. Sci.Technol. 20 (1999) 1097.

[23] M.R. Schure, A.M. Lenhoff, Anal. Chem. 65 (1993) 3024.

[14] M. Minarik, B. Gas, A. Rizzi, E. Kenndler, J. Cap. Electrophoresis 2 (1995) 89.

[15] J.S. Green, J.W. Jorgenson, J. Chromatogr. 478 (1989) 63.

[16] N. Fang, J.W. Li, E.S. Yeung, Anal. Chem. 79 (2007) 5343.

[17] J.K. Towns, F.E. Regnier, Anal. Chem. 64 (1992) 2473.

[18] J.R. Mazzeo, I.S. Krull, in J.P. Landers (Editor), Handbook of Capillary Electrophoresis, CRC, Boca Raton, FL, 1994, p. 495.

[19] C.A. Lucy, N.E. Baryla, K.K.C. Yeung, in M.A.L. Strege, A.L. (Editor), Capillary Electrophoresis of Proteins and Peptides, Humana Press, Totowa, NJ, 2004.

[20] P.G. Righetti, C. Gelfi, B. Verzola, L. Castelletti, Electrophoresis 22 (2001) 603.

[21] J.A. Bullock, L.C. Yuan, J. Microcol. Sep. 3 (1991) 241.

[22] A. Cifuentes, M.A. Rodriguez, F.J. Garcia-Montelongo J. Chromatogr. A 742

(1996) 257.
[23] A. Cifuentes, M. de Frutos, J.M. Santos, J.C. Diez-Masa, J. Chromatogr. 709 (1993) 63.
[24] D. Corradini, A. Rhomberg, C. Corradini, J. Chromatogr. A 661 (1994) 305.
[25] N.A. Guzman, J. Moschera, K. Iqbal, W. Malick, J. Chromatogr. 608 (1992) 197.
[26] J. Bullock, J. Chromatogr. 633 (1993) 235.
[27] V. Rohlicek, Z. Dehil, J. Chromatogr. 494 (1989) 87.
[28] Y.J. Yao, S.F.Y. Li J. Chromatogr. A 663 (1994) 97.
[29] A. Cifuentes, H. Poppe, J.C. Kraak, J. Chromatogr. B 681 (1996) 21.
[30] B. Verzola, C. Gelfi, P.G. Righetti, J. Chromatogr. A 868 (2000) 85.
[31] P.G. Righetti, C. Gelfi, R. Sebastiano, A. Citterio, J. Chromatogr. A 1053 (2004) 15.
[32] D. Corradini, L. Bevilacqua, I. Nicoletti, Chromatographia 62 (2005) S43.
[33] S. Hjertèn, K. Kubo, Electrophoresis 14 (1993) 390.
[34] M. Huang, J. Plocek, M.V. Novotny, Electrophoresis 16 (1995) 396.
[35] J.L. Liao, J. Abramson, S. Hjertèn, J. Capill. Electrophor. 2 (1995) 191.
[36] J.T. Smith, Z. El Rassi, Electrophoresis 14 (1993) 396.
[37] M. Gilges, M.H. Kleemis, G. Schomburg, Anal. Chem. 66 (1994) 2038.
[38] E. Simò-Alfonso, M. Conti, C. Gelfi, P.G. Righetti, J. Chromatogr. A 689 (1995) 85.
[39] M. Iki, E.S. Yeung, J. Chromatogr. A 731 (1996) 273.
[40] H. Lindner, W. Helliger (1997) Capillary electrophoresis in Biotechnology and Environmental Analysis. In: Parvez P, Caudy S, Parvez P, Roland-Gosselin P (eds) Progress in HPLC-CE Series Vol 5. VSP, Utrecht
[41] H. Lindner, W. Helliger, A. Dirschlmayer, M. Jaquemar, B. Puschendorf Biochem. J. 283 (1992) 467.
[42] M.F. Fraga, E. Ballestar, A. Villar-Garea, M. Boix-Chornet, J. Espada, G. Scotta, T. Bonaldi, C. Haydon, S. Ropero, K. Petrie, N.G. Iyer, A. Perez-Rosado, E.

Calvo, J.A. Lopez, A. Cano, M.J. Calasanz, D. Colomer, M.A. Piris, N. Ahn, A. Imhof, C. Caldas, T. Jenuwein, M. Esteller, Nature genetics 37 (2005) 391.

[43] M. Boix-Chornet, M.F. Fraga, A. Villar-Garea, R. Caballero, J. Espada, A. Nunez, J. Casado, C. Largo, J.I. Casal, J.C. Cigudosa, L. Franco, M. Esteller, E. Ballestar, J. Biol. Chem. 281 (2006) 13540.

[44] M. Kato, E. Imamura, K. Sakai-Kato, T. Nakajima, T. Toyo'oka, Electrophoresis 27 (2006) 1895.

[45] G. L. Erny, C. Elvira, J. San Román, A. Cifuentes, Electrophoresis 27 (2006) 1041.

[46] I. Fermo, L. Germagnoli, A. Soldarini, F. Dorigatti, R., Paroni, Electrophoresis 25 (2004) 469.

[47] M.M. Yassine, C.A. Lucy, Anal. Chem. 76 (2004) 2983.

[48] Y.H. Dou, N. Bao, J.J. Xu, F. Meng, H.Y. Chen, Electrophoresis 25 (2004) 3024.

[49] W. Wei, H.X. Ju, Electrophoresis 26 (2005) 586.

[50] K.K.C. Yeung, K.K. Atwal, H.X. Zhang, Analyst 128 (2003) 566.

[51] H.X. Zhang, K.K.C. Yeung, Anal. Chem. 76 (2004) 6814.

[52] M.V. Linden, S.K. Wiedmer, R.M.S. Hakala, M.L. Riekkola, J. Chromatogr. A 1051 (2004) 61.

[53] A. Pontoglio, A. Vigano, R. Sebastiano, L. Maragnoli, P.G. Righetti, C. Gelfi, Electrophoresis 25 (2004) 1065.

[54] D. Corradini, G. Mancinia, C. Bello, J. Chromatogr. A 1051 (2004) 103.

[55] C.Z. Wang, C.A. Lucy, Anal. Chem. 77 (2005) 2015.

[56] C.Z. Wang, C.A. Lucy, Electrophoresis 25 (2004) 825.

[57] S. Ullsten, L. Soderberg, S. Folestad, K.E. Markides, Analyst 129 (2004) 410.

[58] M.N. Albarghouthi, T.M. Stein, A.E. Barron, Electrophoresis 24 (2003) 1166.

[59] A. Zuberovic, S. Ullsten, U. Hellman, K.E. Markides, J. Bergquist, Rapid Commun. Mass Spectrom. 18 (2004) 2946.

[60] V. Sanz-Nebot, F. Benavente, A. Vallverdu, N.A. Guzman, J. Barbosa, Anal.

Chem. 75 (2003) 5220.
[61] C.Q. Shou, C.B. Zhao, C.L. Zhou, Z.L. Zhang, H.B. Jia, G.B. Li, L.R. Chen, Chin. J. Anal. Chem. 32 (2004) 241.
[62] C.Q. Shou, C.L. Zhou, C.B. Zhao, Z.L. Zhang, G.B. Li, L.R. Chen, Talanta 63 (2004) 887.
[63] C. Simo, C. Elvira, N. Gonzalez, J.S. Roman, C. Barbas, A. Cifuentes, Electrophoresis 25 (2004) 2056.
[64] N. Gonzalez, C. Elvira, J. San Roman, A. Cifuentes, J. Chromatogr. A 1012 (2003) 95.
[65] A. Palm, M. Zaragoza-Sundqvist, G.J. Marko-Varga, J. Sep. Sci. 27 (2004) 124.
[66] A. Bossi, L. Castelletti, S.A. Piletsky, A.R. Turner, P.G. Righetti, J. Chromatogr. A 1023 (2004) 297.
[67] W.W.P. Chang, L. Nichols, K. Jiang, L.V. Schneider, Am. Lab. 36 (2004) 8.
[68] M.E. Roche, M.A. Anderson, R.P. Oda, B.L. Riggs, M.A. Strausbauch, R. Okazaki, P.J. Wettstein, J.P. Landers, Anal. Biochem. 258 (1998) 87.
[69] M.X. Li, L. Liu, J.T. Wu, D.M. Lubman, Anal. Chem. 69 (1997) 2451.
[70] R.W. Chiu, J.C. Jimenez, C.A. Monnig, Anal. Chim. Acta 307 (1995) 193.
[71] H. Katayama, Y. Ishihama, N. Asakawa, Anal. Chem. 70 (1998) 2254.
[72] F.B. Erim, A. Cifuentes, H. Poppe, J.C. Kraak, J. Chromatogr. A 708 (1995) 356.
[73] A. Cifuentes, H. Poppe, J.C. Kraak, F.B. Erim, J. Chromatogr. B 681 (1996) 21.
[74] M. Spanila, J. Pazourek, J. Havel, J. Sep. Sci. 29 (2006) 2234.
[75] H. Katayama, Y. Ishihama, N. Asakawa, Anal. Chem. 70 (1998) 2254.
[76] F. Kitagawa, M. Kamiya, Y. Okamoto, H. Taji, et al., Anal. Bioanal. Chem. 386 (2006) 594.
[77] A. Puerta, J. Axen, L. Söderberg, J.J Bergquist, J. Chromatogr. B 838 (2006) 113.
[78] M.H.A. Busch, J.C. Kraak, H. Poppe, J. Chromatogr. A 695 (1995) 287.
[79] Y. Shen, R.D. Smith, J. Microcol. Sep. 12 (2000) 135.

[80] R.D. Sanzgiri, T.A. McKinnon, B.T. Cooper, Analyst 131 (2006) 1034.

[81] W.S. Law, J.H. Zhao, S.F.Y. Li, Electrophoresis 26 (2005) 3486.

[82] E.N. Fung, E.S. Yeung, Anal. Chem. 67 (1995) 1913.

[83] R.S. Madabhushi, Electrophoresis 19 (1998) 224.

[84] M. Chiari, M. Cretich, J.Horvath, Electrophoresis 21 (2000) 1521.

[85] A. Cifuentes, P. Canalejas, A. Ortega, J.C. Diez-Masa, J. Chromatogr. A 823 (1998) 561.

[86] S. Hjertèn, J.Chromatogr. 347 (1985) 191.

[87] K.A. Cobb, V. Dolnìk, M. Novotny, Anal. Chem. 62 (1990) 2478.

[88] M.C. Montes, C. van Amen, J.J. Pesek, J.E. Sandoval, J. Chromatogr. A 688 (1994) 31.

[89] H. Engelhardt, M.M. Cunat-Walter, J. Chromatogr. A 716 (1995) 27.

[90] A. Cifuentes, P. Canalejas, J.C. Diez-Masa J.Chromatogr. A 830 (1999) 423.

[91] M. Chiari, M. Nesi, M. Fazio, P.G. Righetti, Electrophoresis 13 (1992) 690.

[92] D. Schmalzing, C.A. Piggee, F. Foret, E. Carrilho, B.L. Krager, J. Chromatogr. 652 (1993) 149.

[93] D. Belder, A. Deege, H. Husmann, F. Kohler, M. Ludwig, Electrophoresis 22 (2001) 3813.

[94] C. Aguilar, A.J.P. Hofte, U.R. Tjaden, J. Van der Greef, J. Chromatogr. A 926 (2001) 57.

[95] H. Burt, D.M. Lewis, K.N. Tapley, J. Chromatogr. A, 739 (1996) 367.

[96] M. Chiari, L. Ceriotti, G. Crini, M. Morcellet, J. Chromatogr. A 836 (1999) 81.

[97] M. Spanilá, J. Pazourek, J.J. Havel, J. Sep. Sci. 29 (2006) 2234.

Chapter 2 :

Determination of oxalyl-coenzyme A decarboxylase activity in *Oxalobacter formigenes* and *Lactobacillus acidophilus* by capillary electrophoresis in a PEI-coated capillary

1. INTRODUCTION

In humans, the absorption of oxalic acid by diets occurs mainly in the colon; the strong ability of oxalate as chelator of cations, calcium in principal, is the basis of oxalate accumulation which can result in a number of pathologic conditions such as: hyperoxaluria, urolithiasis, renal failure, etc. [1]. The oxalate degrading activity of colonic anaerobic bacteria has been widely considered for the possible contribution in regulating the intestinal oxalate homeostasis [2]; in particular, the microorganism *Oxalobacter formigenes* found in the gastrointestinal tract of vertebrates, has been shown to depend totally on oxalate metabolism for energy and its role in scavenging dietary oxalate has been demonstrated [3–5]. In this microorganism, oxalyl-coenzyme A decarboxylase (OXC) is the key enzyme in the catabolism of the highly toxic oxalate, catalysing the decarboxylation of oxalyl-coenzyme A (Ox-CoA) to formyl-coenzyme A (For-CoA) [6]. The structures of Ox-CoA and For-CoA and the scheme of catabolism of oxalate by *O. formigenes* are reported in Fig. 2.1. Besides *O. formigenes*, several bacteria have been recognized in intestinal tract as oxalate-degraders [7]. Furthermore, bacteria industrially employed as probiotics have shown evidence for a potential oxalate-degrading activity [8] and they are now objects of study as potential food additives in the prevention of oxalate-related diseases. The OXC activity in bacteria is conventionally screened by spectrophotometric methods where the decarboxylation of the substrate is estimated by the formate amount yielded as the result of coupled reactions involving, eventually, the reduction of NAD to NADH [6]. The main drawback of these coupled methods is the low specificity of analysis due to the complexity of the enzymatic reaction mixture [9].

The required high selectivity for reliable and fast determinations of enzymatic activity can be fulfilled by applying suitable separation methods; among these, capillary electrophoresis (CE) has shown to be very attractive for the rapid analysis times, automation of the analytical procedure and small consumption of both samples and reagents. As recently reviewed by Glatz [10], CE can be exploited as an efficient separation technique for the quantitation of reaction product(s) or substrate(s) after

the enzyme reaction is occurred (off-line assay).

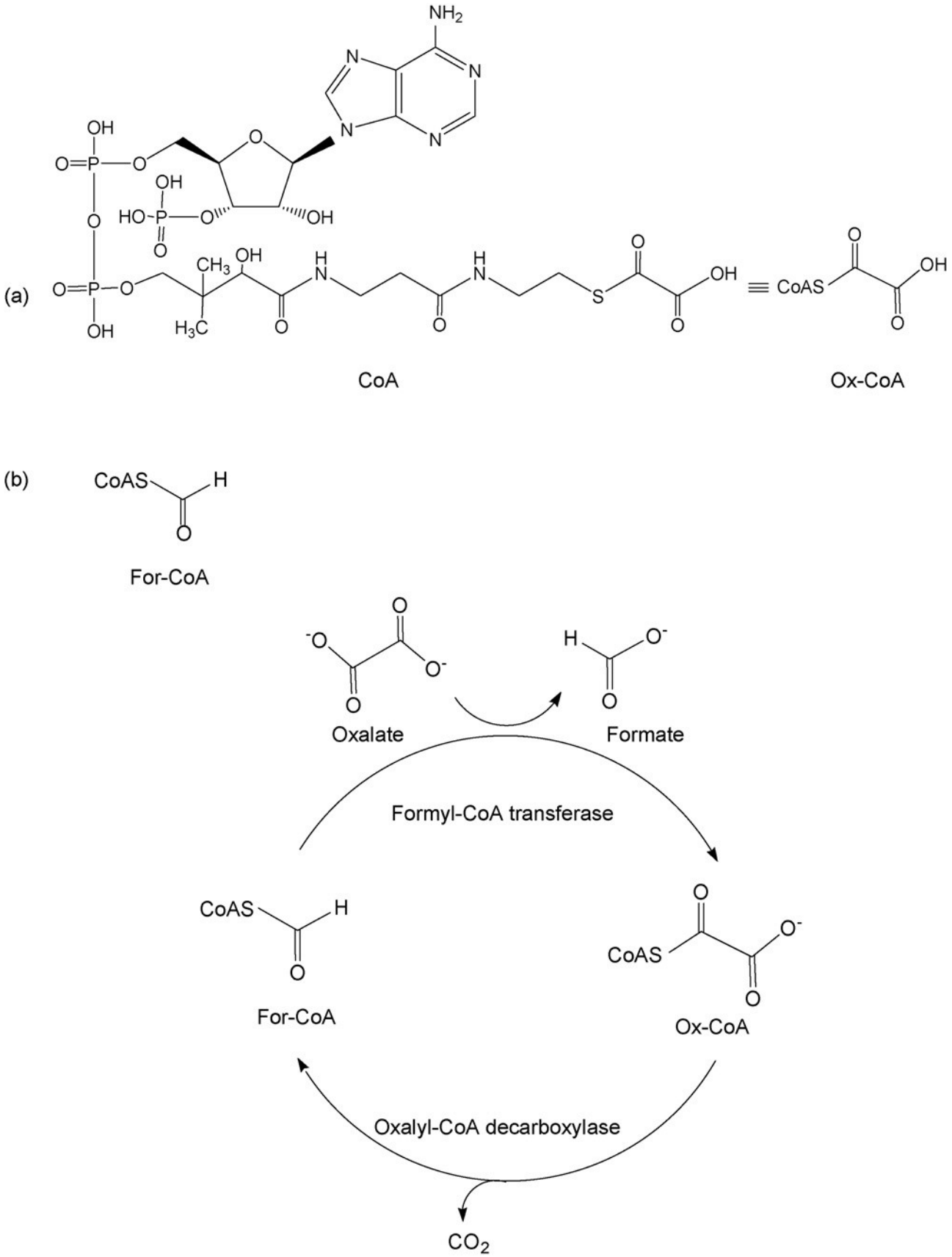

Fig. 2.1. Structures of oxalyl-CoA (a), formyl-CoA (b) and catabolic pathway of oxalate by *O. formigenes*.

Besides these classic approaches, enzymatic reactions can be also advantageously performed in CE by separately introducing inside the capillary both the enzyme and substrate(s) and giving them the possibility to react with each other by applying the electrical field. By exploiting the mobility differences, the products of the enzymatic reaction obtained on-line, can be separated and thus quantified, in a same run (on-line assay).

In a previous paper, an off-line CE method was proposed in evaluating the OXC activity in *Bifidobacterium lactis*, a probiotic bacterium widely used in dairy fermented products and in pharmaceutical preparations [8]. Recent evidences of the efficacy of hyperoxaluria treatment with a lactic acid bacteria mixture containing the probiotic *Lactobacillus acidophilus* [11,12], suggested the determination of its oxalate-degrading activity. An "in vitro" screening of this activity was carried out on several *Lactobacillus* strains isolated from functional foods and pharmaceutical preparations. To this regard CE using a polyethylenimine (PEI) coated capillary [13], was applied for the first time to the determination of Formyl-CoA transferase activity and oxalyl-CoA decarboxylase activity. The method provided a reversed electroosmotic flow (from cathode to anode) and allowed for a fast separation of the reaction substrate Ox-CoA and the product For-CoA [14]. The previously proposed CE method has been implemented, validated and applied to the assessment of the activity of recombinant OXC from *L. acidophilus* LA 14 and a comparison with the activity of OXC from *O. formigenes* DMS 4420, was carried out. The kinetic parameters of oxalyl-CoA decarboxylase were finally estimated in both the studied bacteria [15].

2. EXPERIMENTAL

2.1. Materials

Polyethylenimine (PEI), phthalic acid and dimethyl sulfoxide (DMSO) (the marker of electroosmotic flow), were provided by Sigma–Aldrich (Milan, Italy). Hydrogen phosphate anhydrous sodium salt, sulfuric acid, sodium hydroxide and all the other chemicals of analytical grade, were purchased from Carlo Erba Reagenti (Milan, Italy). Water used for the preparation of solutions and running buffers, was purified by a Milli-RX apparatus (Millipore, Milford, MA, USA).

2.2. Standard substances

The standard substance Ox-CoA is not commercially available and it was synthesized by reaction of coenzyme A with thiocresoxalic acid following a literature procedure [16]. The final product, characterized by NMR, was titrated by a spectrophotometric assay (UV absorbance at 590 nm) using an enzymatic method (Oxalate Diagnostic, Prisma, Milan, Italy) based on the oxidation of oxalate, by oxalate oxidase [17]. Briefly, an accurately weighted amount of the synthesized Ox-CoA was dissolved in water and 50 L aliquot of the obtained solution was neutralized to pH 7.0 by adding a 5 μL volume of sodium hydroxide (0.1 M). After stirring, the mixture was stored at 37◦C for 15 min in the presence of the enzymatic reagents from the Oxalate Diagnostic kit; finally the mixturewas acidified to pH 5.0 by addition of hydrochloric acid (0.1 M). The concentration of synthesized Ox-CoA was determined by comparison with a reference standard solution of oxalate. The Ox-CoA solution was then diluted and stored at the final concentration of 2.0mM at the temperature of −80 ◦C.

Formyl-CoA was synthesized by ester interchange between CoA and thiocresyl formate [18]; the identity of the obtained compound was confirmed by NMR spectrum. The synthesized For-CoA was not further purified nor titrated, because it was used as standard only for qualitative analysis.

2.3. Apparatus

Electrophoretic experiments were performed on a BioRad Biofocus 2000 instrument from BioRad (Hercules, CA, USA). The data were collected on a personal computer equipped with the devoted BioRad integration software. The separations were carried out on a PEI-coated capillary of 50 μm internal diameter (ID) with a total length of 36 cm (effective length 31.5 cm). The procedure for the coating of the capillary using PEI was based on a published method [13]. In order to obtain high repeatability of migration times, the capillary was rinsed between the runs with water (2 min) and separation buffer (2 min). The electrophoretic runs were performed at a constant voltage of 10 kV (anodic detection) with controlled temperature (25 ◦C). The samples were injected hydrodynamically using a pressure of 2 psi s (1 psi = 6894 Pa); the detection wavelength was 254 nm.

2.4. Solutions

Phosphate buffer used as the background electrolyte (BGE) was prepared at the concentration of 50 mM in water and the pH was adjusted at the desired value using a 0.1M aqueous solution of phosphoric acid. Sulfuric acid aqueous solution was used at the concentration of 0.1N. The experiments for the evaluation of OXC activity were performed on solutions of the substrate (Ox-CoA) in a buffer constituted of phosphate (0.1 M; pH 6.8), thiamine pyrophosphate (60 μM) and $MgCl_2$ (6.0 mM).

2.5. Calibration curve

Linearity of the response was investigated for the substrate (Ox-CoA) in the concentration range of 0.005–0.650mM in the buffer solution by using phthalic acid as internal standard (final concentration of 0.60 mM). Triplicate injections were made for each of the samples and the mean corrected peak area (area/migration time) ratios of the analyte to that of the internal standard were plotted against the concentrations to obtain the calibration graph by linear regression analysis.

2.6. Oxalyl-CoA decarboxylase reaction

The evaluation of OXC activity was carried out by measuring the consumption of the substrate Ox-CoA. The reaction mixture was constituted of the substrate Ox-CoA dissolved in the buffer (see Section 2.4). The reaction started by adding the soluble fraction (100 ng/μL protein) of a recombinant *Escherichia coli* clone overexpressing *L. acidophilus* LA 14 OXC enzyme. Likewise, the reaction was performed using the soluble fraction of a recombinant *E. coli* clone overexpressing *O. formigenes* DSM 4420 OXC enzyme (100 ng/L protein).

Each mixture (total volume of 165 μL)was incubated at 37◦C for a period ranging from 5 to 90 min (*L. acidophilus* LA 14) or 30–120 s (*O. formigenes* 4420) and quenched with 16.5 μL of sulfuric acid (0.1N). Before CE analysis, the reaction mixtures were neutralized by adding 20 μL of NaOH (0.1 M) containing phthalic acid (0.60 mM) as the internal standard.

2.7. Kinetic analysis of oxalyl-CoA decarboxylase

The kinetic studies were performed using the cytoplasmatic extracts of recombinant *E. coli* clones overexpressing either *L. acidophilus* LA 14 oxalyl-CoA decarboxylase or *O. formigenes* DSM 4420 oxalyl-CoA decarboxylase. The evaluation of the Ox-CoA degradation rate was carried out by analysing the different reaction mixtures containing different substrate Ox-CoA levels, ranging within 0.010–0.600 mM.

The data were fitted to the single-site Michaelis–Menten (hyperbolic substrate concentration dependence) and autoactivation (sigmoidal substrate concentration dependence) models. The autoactivation model is expressed by the Hill equation: $v = V_{max}[S]^h/(k' + [S]^h)$, where v is the rate of the metabolic reaction, $[S]$ the substrate concentration, V_{max} the maximum rate, k' is a constant of the autoactivation model that is equivalent to Michaelis–Menten K_m for $h = 1$, where h is the Hill coefficient.

Standard parameters such as the determination coefficient (r^2) and standard errors of the parameter estimates were used to determine the quality of a fit to a specific model. Both fits and determination of the apparent enzyme kinetic parameters, K_m,

V_{max}, k' and h, were calculated by non-linear regression analysis using GraphPad Prism version 4.0 (GraphPad software, San Diego, CA, USA).

3. RESULTS AND DISCUSSION

The evaluation of oxalyl-CoA decarboxylase and formyl-CoA transferase activity in oxalate-degrading bacteria can be conveniently determined by the enzymatic mixture variations in concentration of both Ox-CoA and For-CoA which perform as substrate/product in the oxalate degradation cycle (Fig. 2.1). A capillary electrophoretic approach has been previously applied in our laboratory to these evaluations in *L. acidophilus*; in particular the analysis of the anionic species Ox-CoA and For-CoA was carried out under co-electroosmotic flow mode [14]. The proposed CE method has been implemented, validated and applied to estimate the kinetic parameters of OXC from *L. acidophilus* LA 14 and *O. formigenes* DSM 4420.

3.1. Method development

The analysis of anionic species under reversed EOF was found to be advantageous because of the shorter analysis time and improved peak shapes obtained in comparison to the conventional counter-electroosmotic migration [19,20]. In general, the inversion of the EOF is achieved by introducing cationic additives into the BGE to provide a dynamic coverage of the inner capillary silica surface that results positively charged. As previously mentioned, Righetti et al. summarized the different approaches in quenching and/or modulating the EOF by using different classes of compounds as BGE additives [21]. Most commonly, surfactants such as hexadecyltrimethylammonium bromide (CTAB) even if used at concentrations below the critical micelle concentration (cmc), reverse the EOF direction. In our preliminary experiments however, the addition of CTAB to the electrophoretic BGE resulted to be useless in analysis of Ox-CoA and For-CoA, likely due to their electrostatic as well as hydrophobic interactions with the surfactant monomers. Alternatively, the use of a capillary coated with a cationic layer, allowed the EOF to be reversed, avoiding the addition to the BGE of interfering additives. In this regard, PEI resulted to be a useful compound for the preparation of permanent coated capillaries: in fact as it has been previously proposed [13], PEI is a polycationic branched polymer able to be

permanently adsorbed by the silica surface of the capillary wall. Detailed studies were reported on the EOF variations in PEI-coated capillaries using different running buffer nature and pH [13,22–25]. In the present study, a fused silica capillary was modified by adsorption of a 10% (w/v) PEI aqueous solution and it was used, in the presence of a BGE consisting of phosphate running buffer (50 mM, pH 7.0), in the analysis of actual enzymatic mixtures containing Ox-CoA and For-CoA. By applying a constant voltage of 10 kV (anodic detection), the obtained current was about 35μA and the electroosmotic mobility, measured using DMSO (0.01% aqueous solution) as the neutral marker, was determined to be -6.0×10^{-5} cm^2 s^{-1} V^{-1}. Under these conditions the complete separation of Ox-CoA and For-CoA was accomplished in less than 12 min (Fig. 2.2)

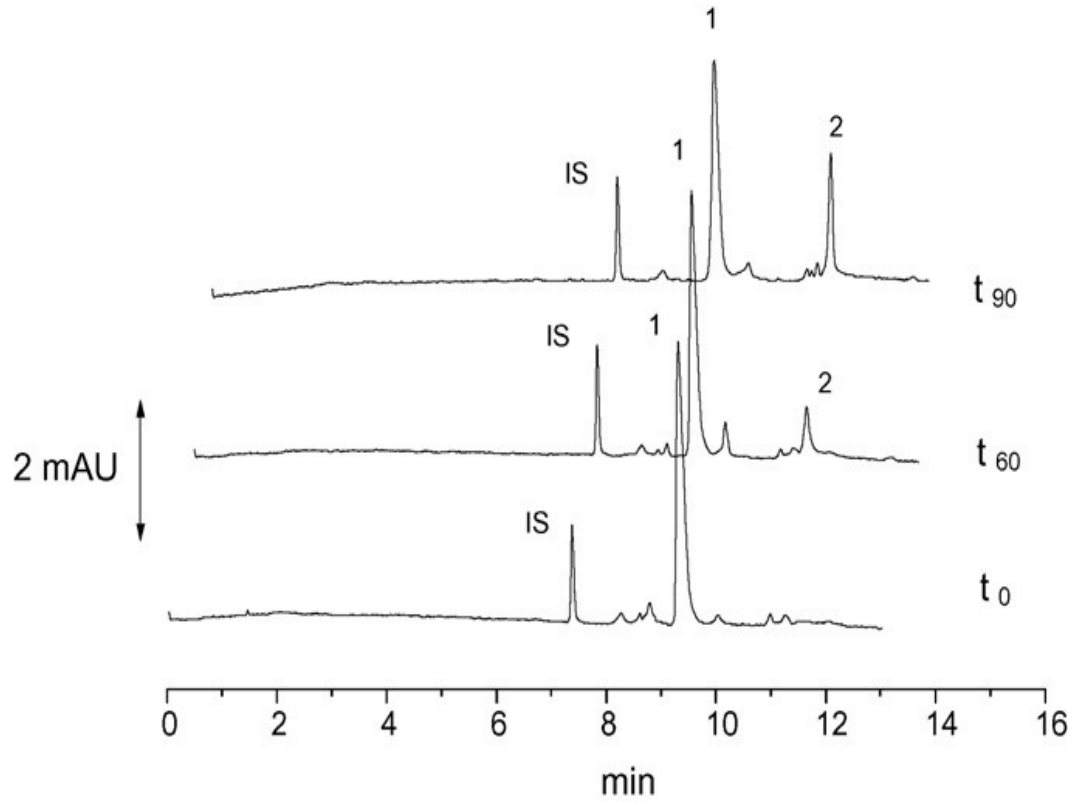

Fig. 2.2. Electropherograms of enzymatic reaction mixtures in presence of OXC from *L. acidophilus* LA 14 after different incubation times (0, 60 and 90 min); the initial concentration of Ox-CoA was 0.150 mM. *Conditions*: PEI-coated capillary (effective length 31.5 cm; 50 μm ID); the BGE is a 50mM phosphate buffer (pH 7.0); applied voltage −10 kV; wavelength at 254 nm; hydrodynamic injection at 2 psi s; capillary temperature at 25 ◦C. *Symbols*: IS, internal standard; (1) Ox-CoA; (2) For-CoA.

3.2. Method validation

3.2.1. Linearity and sensitivity

Calibration curve was obtained by plotting the corrected peak area ratios of Ox-CoA to the internal standard (phthalic acid) (*Y*), versus the corresponding concentrations of the analyte (*C*; mM). By linear regression analysis the following equation was obtained: $Y = 40.962\ (\pm 0.381)C + 0.291\ (\pm 0.117)$; $r^2 = 0.999$. The sensitivity data at the detection wavelength of 254 nm estimated as LOD (S/N = 3) and LOQ (S/N = 10) were found to be 1.5 and 5.0μM (RSD = 3.2%; $n = 3$), respectively.

3.2.2. Selectivity and reproducibility

Identification of the studied analytes was performed by comparison of the migration

times obtained in actual samples with those of the standard solutions. Furthermore, spiking experiments (standard addition method) were performed to confirm the peak identity.

The repeatability of the separation system was evaluated by replicated analysis of solution (0.150 mM) of Ox-CoA and For-CoA; the relative standard deviations of migration time were 1.07% and 1.05% (n = 5, intra-day) and 3.56% and 3.72% (n = 15, inter-day), for Ox-CoA and For-CoA, respectively. The RSD% of the corrected peak area ratio (analytes to internal standard) were 1.02% and 0.98% (n = 5, intra-day) for Ox-CoA and For-CoA, respectively, and it was found to be less than 6.0% over a three consecutive days experiments (n = 15).

3.2.3. Recovery studies

The accuracy of the method was evaluated by comparing the quantitative results obtained by the analysis of actual samples (enzymatic reaction mixtures) using the proposed CE method with those obtained by applying a standard spectrophotometric method based on the coupled assay described in experimental section (see Section 2.2). Precisely, aliquots of the stock solution of the substrate Ox-CoA corresponding to about 0.300 mM were mixed with the reaction cofactors and added, in the order with sulfuric acid solution (0.1N) and OXC from *O. formigenes* DSM 4420. Under these conditions, the pH requirement for the enzymatic reaction was not fulfilled and the oxalate degradation activity did not occur. Afterward, the samples were subjected to analysis of Ox-CoA using both the techniques (CE and spectrophotometric coupled assay); the obtained results (mean of five independent samples) were 0.301mM (RSD 0.49%) and 0.307mM (RSD 0.20%), respectively. The variance ratio F-test values calculated at 95% confidence level did not exceed the tabulated value, thus indicating no significant difference between the two applied methods.

3.3. Application to kinetic monitoring of OXC from O. formigenes DSM 4420 and L.acidophilus LA 14

The time course of substrate degradation by OXC from both of the bacteria was determined by analysis of Ox-CoA carried out at different times of the enzymatic reactions; electropherograms of the analysed actual enzymatic mixtures using *L. acidophilus* LA 14 at time zero and after 60 and 90 min are reported in Fig. 2.2. The corrected peak area ratios (remaining substrate versus internal standard) were plotted against the reaction time to obtain the degradation kinetics for both the bacteria (Fig. 2.3a and b). The concentration of Ox-CoA in these experiments was 0.150 mM. As expected, owing to the demonstrated dependence on oxalate metabolism for energy, the profiles of degradation of Ox-CoA showed that *O. formigenes* DSM 4420 OXC activity is significantly higher than that observed in *L. acidophilus* LA 14. However, although the latter showed to be not specifically involved in oxalate metabolism, the obtained results confirmed its role as oxalate-degrading microorganism. For a more in depth characterization of OXC activity, kinetic parameters were also estimated.

3.3.1. Kinetic parameters of OXC from O. formigenes DSM 4420

The time course evaluated in *O. formigenes* DSM 4420 (Fig. 2.3a), suggested that the degradation of the substrate Ox-CoA completely occurred within 2 min, thus the initial rate (v_0) was estimated by quenching the enzymatic reaction after 5 s. Under this condition, the observed decrease in the peak area of the substrate was corresponding to about 5%. Five different Ox-CoA levels within the concentration range 0.010–0.310 mM, were reacted with the enzyme OXC in triplicate; after 5 s the reactions were quenched and the remaining Ox-CoA amount (expressed as μmol) for each of the levels, was determined by the validated CE method using external standardization. The obtained data (mean of three measurements) were used to evaluate the initial rate of the metabolic reaction at different substrate concentrations. The kinetic parameters of OXC in the considered substrate concentration range were obtained by the Michaelis–Menten plot as shown in Fig. 2.4.

The curve fitting to $v = V_{max}[S]/(K_m + [S])$ gave a V_{max} of 8.47±0.51 μmol/min/mg and

a K_m of 34.3±6.6M, with a r^2 value of 0.98. The obtained values were basically in agreement with those previously reported [9].

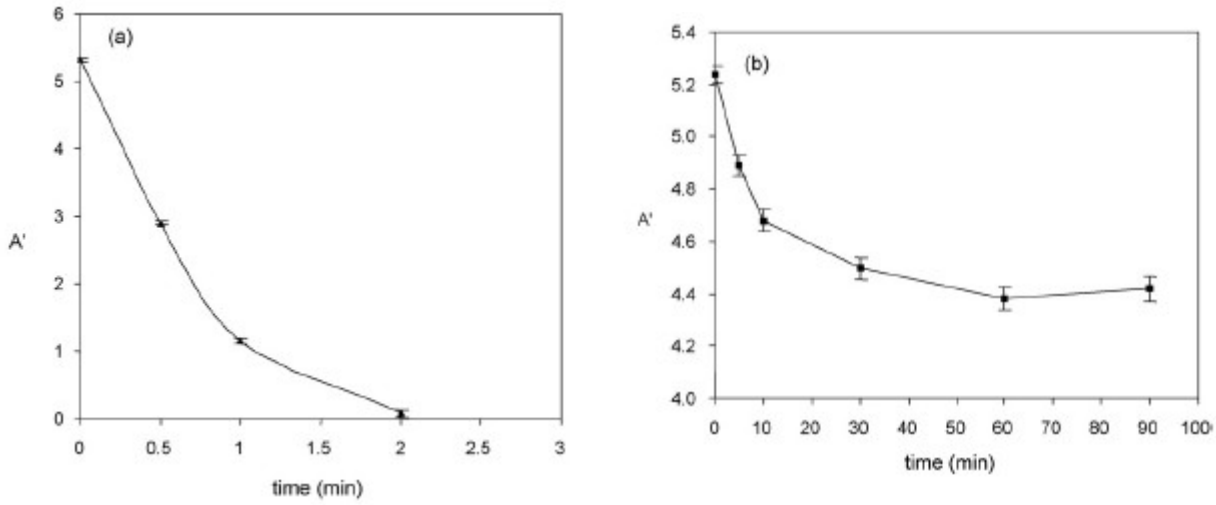

Fig. 2.3. Degradation kinetics of Ox-CoA by OXC from *O. formigenes* DSM 4420 (a) and from *L. acidophilus* LA 14 (b) as estimated by CE method. The concentration of Ox-CoA was 0.150 mM. *A*' is the corrected peak area ratio.

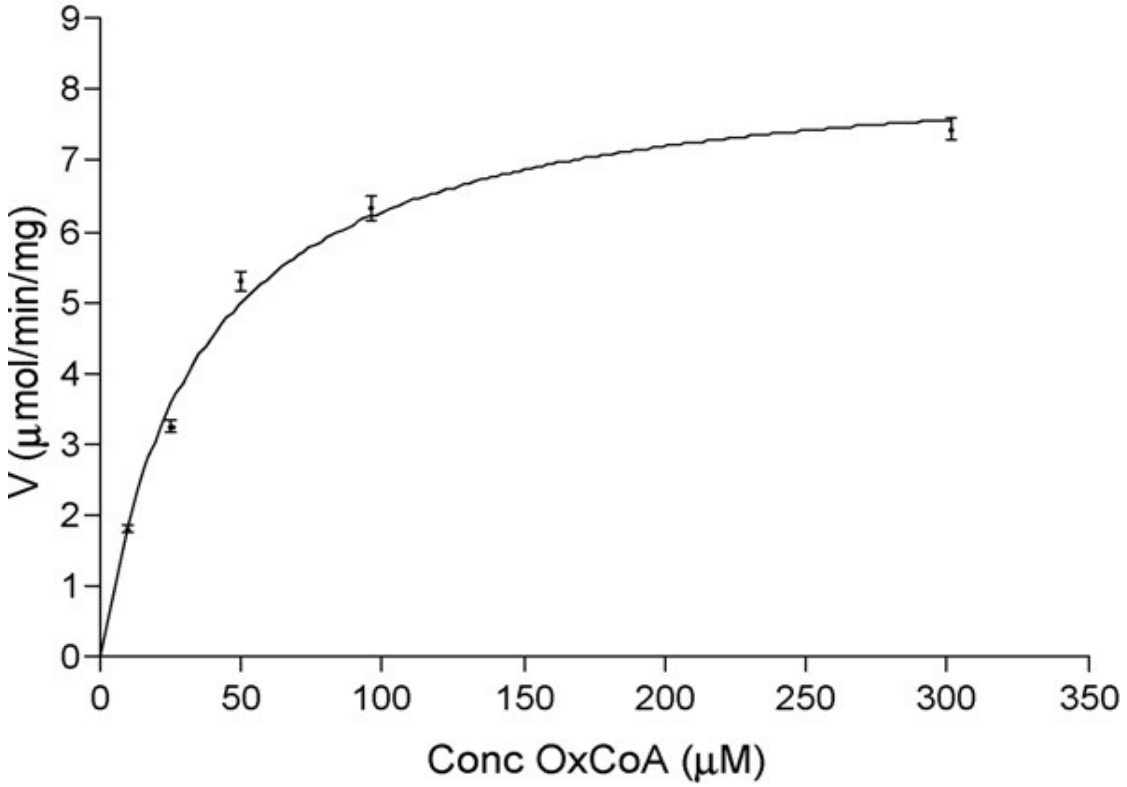

Fig. 2.4. Ox-CoA degradation rate vs. Ox-CoA concentration for OXC from *O. formigenes* DSM 4420 fitted with the Michaelis–Menten model.

3.3.2. Kinetic parameters of OXC from L. acidophilus LA 14

The kinetic parameters were estimated in *L. acidophilus* LA 14 by following the same experimental approach as for *O. formigenes* DSM 4420; however, since *L. acidophilus* LA 14 had shown a slower time course, a ~5% degradation of the initial substrate amount was achieved after 5 min of incubation. Seven different Ox-CoA levels within the concentration range of 0.037–0.574mM were reacted with the enzyme in triplicate and the remaining Ox-CoA amount (µmol) for each of the levels, was determined by the CE method. The kinetic parameters of OXC in the studied substrate concentration range were obtained by curve fitting to $v = V_{max}[S]h/(k + [S]h)$ as shown in the graph of Fig. 2.5. Since the equation fitted with a sigmoidal curve, a positive cooperativity between enzyme and substrate was hypothesized. The best fitting of the curve was found to be at h value of 4, where h is the number of cooperative binding sites. Under these fitting conditions, a V_{max} of 0.0383±0.00134µ

mol/min/mg and a *k*' of 82.6±4.2 μM were found. The good determination coefficient (r^2 value of 0.97) and the obtained high repeatability of the system suggested that, even using a relatively low number of experimental points in the lowconcentration region, the obtained enzyme kinetic parameters can be fairly accepted. Fig. 2.5. Ox-CoA degradation rate vs. Ox-CoA concentration for OXC from *L. acidophilus* LA 14 fitted with the Hill equation model. The pronounced differences in the kinetic parameter values reported for the oxalyl-CoA decarboxylase activity from the two studied bacteria, confirmed the lower oxalate-degrading activity in *L. acidophilus*, in agreement with its known ability to use substrate other than oxalate for growth. Furthermore, the supposed positive cooperativity and the putative presence of four interacting binding sites suggested a multimeric (presumably tetrameric) nature of *Lactobacillus* OXC. It is noteworthy that the crystal structure of *O. formigenes* OXC showed a tetrameric arrangement [9].

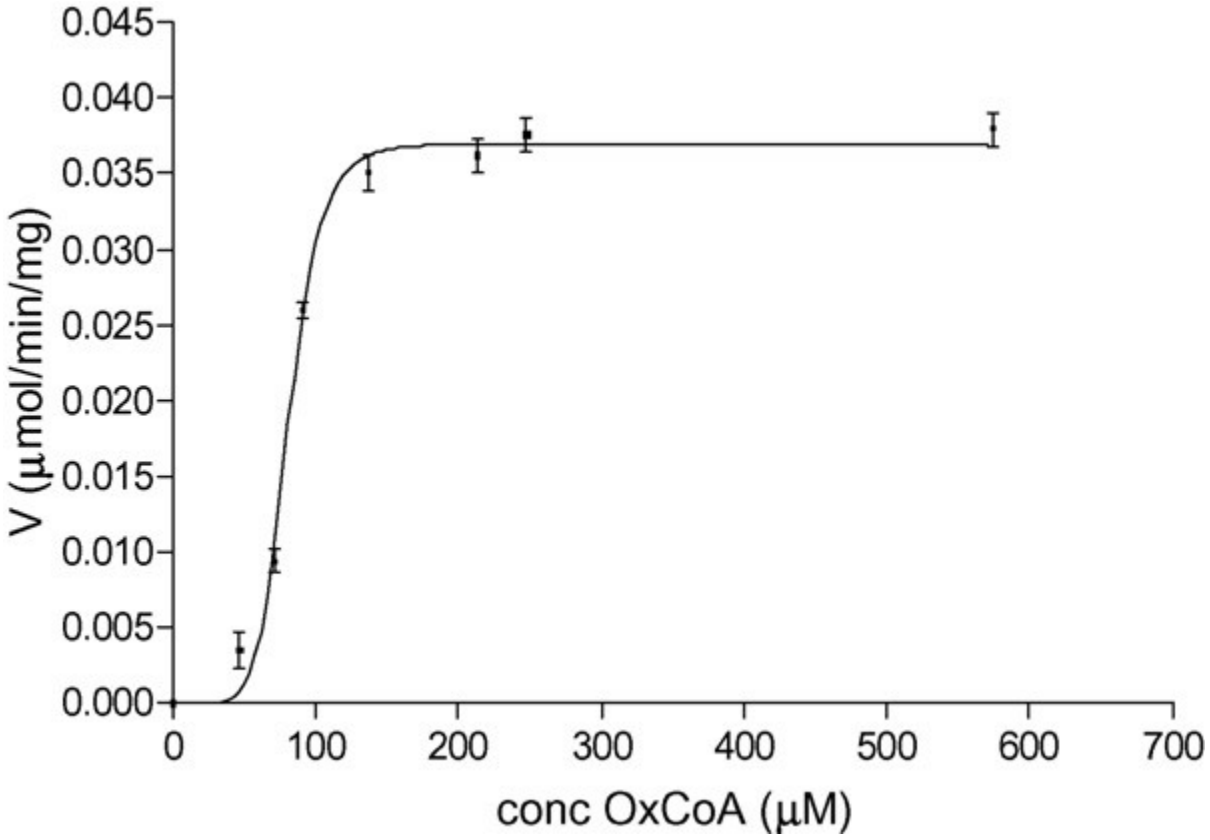

Fig. 2.5. Ox-CoA degradation rate vs. Ox-CoA concentration for OXC from *L. acidophilus* LA 14 fitted with the Hill equation model.

4. Conclusion

A previously developed CE method has been implemented and validated for the quantitation of Ox-CoA in a wide range of concentration in order to be applied in evaluating the consumption of the toxic compound oxalate by the oxalate-degrading bacteria *O. formigenes* DSM 4420 and *L. acidophilus* LA 14. The method has allowed the determination of kinetic parameters of OXC from both the bacteria, showing that although *Lactobacillus* provided a lower oxalate breakdown than *Oxalobacter*, the first could be a potentially useful probiotic in the prevention of diseases related to oxalate. The proposed CE method showed to be reliable and easy to apply thus representing a suitable and convenient alternative to the spectrophotometric method of analysis suffering for poor selectivity.

In particular, the use of PEI coating resulted to be essential in achieving fast and reproduciblw analysis. In fact the co-electrosmotic flow migration of the analysed solutes represents a key innovation in this off-line CE assay; a good throughput is obtained and this allows for a relatively high number of samples to be processed. This achievement was the base for the development of the study on kinetic parameters of *L. acidophilus* LA 14 and *O. formigenes* DSM 4420. In particular the kinetic data obtained for *O. formigenes* DSM 4420, were found to be in good agreement with those reported in the literature and obtained by applying a gradient elution HPLC method.

References

[1] H.E. Williams, L.H. Smith, Am. J. Med. 45 (1968) 715.

[2] M.J. Allison, C.M. Hook, D.B. Milne, S. Gallagher, R.V. Clayman, J. Nutr. 116 (1986) 455.

[3] K.A. Dawson, M.J. Allison, P.A. Hartman, Appl. Environ. Microbiol. 40 (1980) 833.

[4] H. Sidhu, M.E. Schmidt, J.G. Cornelius, M.E. Thamilselvan, S.R. Khan, A. Hesse, A.B. Peck, J. Am. Soc. Nephrol. 10 (1999) S334.

[5] M. Hatch, J. Cornelius, M. Allison, H. Sidhu, A. Peck, R.W. Freel, Kidney Int. 69 (2006) 691.

[6] A.L. Baetz, M.J. Allison, J. Bacteriol. 171 (1989) 2605.

[7] S. Hokama, C. Toma, M. Iwanaga, M. Morozumi, K. Sugaya, Y. Ogawa, Int. J. Urol. 12 (2005) 533.

[8] F. Federici, B. Vitali, R. Gotti, M.R. Pasca, S. Gobbi, A.B. Peck, P. Brigidi, Appl. Environ. Microbiol. 70 (2004) 5066.

[9] C.L. Berthold, P. Moussatche, N.G.J. Richards,Y. Lindqvist, J. Biol. Chem. 280 (2005) 41645.

[10] Z. Glatz, J. Chromatogr. B 841 (2006) 23.

[11] C. Campieri, M. Campieri, V. Bertuzzi, E. Swennen, D. Matteuzzi, S. Stefoni, F. Pirovano, C. Centi, S. Ulisse, G. Famularo, C. De Simone, Kidney Int. 60 (2001) 1097.

[12] J.C. Lieske, D.S. Goldfarb, C. De Simone, C. Reigner, Kidney Int. 68 (2005) 1244.

[13] F.B. Erim, A. Cifuentes, H. Poppe, J.C. Kraak, J. Chromatogr.A 708 (1995) 356

[14] S. Turroni, B. Vitali, C. Bendazzoli, M. Candela, R. Gotti, F. Federici, F. Pirovano, P. Brigidi, J. Appl. Microbiol. 103 (2007) 1600

[15] C. Bendazzoli, S. Turroni, R. Gotti, S. Olmo, P. Brigidi, V. Cavrini, J. Chromatogr. B, 854 (2007) 350-356.

[16] J.R. Quayle, Biochim. Biophys. Acta 57 (1962) 398.

[17] M.F. Laker, A.F. Hofmann, B.J. Meeuse, Clin. Chem. 26 (1980) 827.
[18] P.C. Bax, W. Stevens, Recl. Trav. Chim. Pays-Bas Belg. 89 (1970) 265.
[19] A.J. Zemann, J. Chromatogr. A 787 (1997) 243.
[20] S.M. Masselter, A.J. Zemann, J. Chromatogr. A 693 (1995) 359.
[21] P.G. Righetti, C. Gelfi, R. Sebastiano, A. Citterio, J. Chromatogr. A 1053 (2004) 15.
[22] F.B. Erim, J. Chromatogr. A 768 (1997) 161.
[23] A. Cifuentes, H. Poppe, J.C. Kraak, F.B. Erim, J. Chromatogr. B 681 (1996) 21.
[24] E. Cordova, J. Gao, G.M. Whitesides, Anal. Chem. 69 (1997) 1370.
[25] M. Spanila, J. Pazourek, J. Havel, J. Sep. Sci. 29 (2006) 2234.

Chapter 3 :

Penicillin G acylase as chiral selector in CE using a pullulan-coated capillary

1. INTRODUCTION

Proteins, widely used as chiral selectors in LC (HPLC), can be favorably applied also in CE as free solution pseudostationary phases for analytical enantioseparations, as reviewed by Lloyd *et al.* [1, 2], Haginaka [3], and Tanaka and Terabe [4]. The major advantage of this approach is the opportunity to dissolve the proteins in the BGE, thus avoiding immobilization procedures to the silica surface of the stationary phase. The critical problem in the use of proteins as well as of other UV-absorbing chiral selectors dissolved in the electrophoretic BGE is the strong interference with the detection of the analytes resulting in low sensitivity; furthermore, phenomena of ionic suppression limit the opportunity for CE-MS hyphenation. To overcome these drawbacks, the partial filling technique can be effectively and smartly applied. This approach, introduced by Valtcheva *et al.* [5] has attracted great attention as demonstrated by the number of applications using different types of chiral selectors such as: proteins and glycopeptides with UV detection [1–16], CDs, proteins and crown ethers with MS detection [17–19]. Briefly, in partial filling, the running buffer supplemented with the chiral selector is introduced into the capillary by a gentle hydrodynamic pressure avoiding the plug containing the selector to reach the detection window. The subsequent analysis is carried out by a countercurrent mode; namely, under the applied electric field, the selector zone should migrate toward the injection end and thus never reaching the detection window. On the contrary, the analytes, migrating in opposite direction, can be detected without interference from the UV-absorbing chiral selector. Recently, [13, 14] the application of partial filling in co-EOF mode has been shown using glycopeptide antibiotics as chiral selectors. As reported, the plug of the chiral selector is carried to the detector by EOF in the same direction of the analytes; under these conditions, the separation window is limited by the possible interference of the selector zone with those of the studied solutes. Nevertheless, successful enantioresolutions were obtained by a suitable choice of the length of the selector plug.

In the present study [20], penicillin G acylase (PGA), an *N*-terminal nucleophile

hydrolase, was applied for the first time as a chiral selector in free solution CE in partial filling mode for the resolution of chiral acidic compounds. PGA catalyzes the hydrolysis of penicillin G to phenylacetic acid and 6-aminopenicillanic acid and it is well known for its industrial application in the production of the β-lactamic nucleus, which is a building block in the synthesis of semisynthetic penicillins [21]. Moreover, the enzyme is capable of accepting a wide range of structurally different compounds, including phenylacetylated derivatives of anilines, alcohols, α- and β-amino acids, and it is able to selectively recognize the side chain according to its chirality. This has suggested the investigation of PGA as chiral selector in HPLC [22]. PGA-based chiral stationary phases (CSPs) have been developed using different chromatographic supports and immobilization reactions [23, 24]. As expected, PGA proved to be a good chiral selector only for acidic compounds, products of the enzyme catalyzed reactions. The chiral recognition properties of PGA-CSPs have been investigated and the enantioresolution of 2-aryloxyalkanoic and 2-arylpropionic acids was obtained [25, 26]. These promising results led us to investigate PGA as a chiral selector in free solution CE, a highly efficient technique which requires minor enzyme consumption.

For the development of a reliable enantioselective method based on PGA, the use of coated capillaries was found to be essential in order to (i) minimize the adsorption of the protein by the capillary wall, (ii) suppress the EOF avoiding both selector and analytes to migrate in the same direction, (iii) obtain adequate reproducibility. To satisfy these requirements, pullulan, a homopolysaccharide consisting of maltotriose and maltotetraose units with both a-(1→4) and a-(1→6) linkages [26] was used for the first time in the generation of a permanent coating of the inner capillary. The coverage of the free silanol groups by the developed coating significantly reduced the EOF in a wide pH range and showed long-term stability. Racemic ketoprofen was selected as a model acidic compound in optimization of running buffer pH, PGA concentration, and length of protein plug used in partial filling. Under the optimum conditions, a series of chiral acidic drugs resulted to be baseline enantioresolved in a

short analysis time.

2. EXPERIMENTAL

2.1. Materials

Fused-silica capillaries (50 mm id, 48.5 cm total length, 40 cm length to the detector) were from Composite Metal Service (Ilkley, UK). Glycidiloxypropyltrimethoxysilane, boron trifluoride diethyletherate (BF_3), and penicillin acylase (PGA) from *Escherichia coli*, 37 U/mg protein (56 mg/mL) solution in phosphate buffer (pH 7.5) were from Fluka (Buchs, Switzerland). DMSO (Aldrich) was diluted with water (0.1%, v/v) and the solution was used as the marker of the EOF. *Rac*-ketoprofen, DL-β-phenyllactic acid, *rac*-fenoprofen calcium salt hydrate, *rac*-flurbiprofen, *rac*-suprofen, and pullulan from *Aeurobasidium pullulans* were from Sigma (Milan, Italy). (*S*)-Ketoprofen and (±)-4-bromomandelic acid were from Aldrich (Milan, Italy). 2-(4-Chlorophenoxy)-phenylacetic acid and 2-(4-chlorophenoxy)-phenylpropionic acid with the relative (*S*)-enantiomers were a kind gift from Professor P. Tortorella (University of Bari, Italy). Single enantiomer of (*S*)-flurbiprofen was a kind gift from Professor C. Bertucci (University of Bologna, Italy). Phosphoric acid, sodium hydroxide, sodium carbonate, and all the other chemicals were from Carlo Erba Reagenti (Milan, Italy). Water used for the preparation of solutions and running buffers was purified by a Milli-RX apparatus (Millipore, Milford, MA, USA).

2.2. Solutions

Sodium phosphate running buffers, used in the optimization experiments as well as in EOF mobility measurement, were prepared in water from anhydrous disodium phosphate, and the pH was adjusted at the desired value by addition of phosphoric acid solution. Solutions of the chiral selector (PGA) were prepared by suitable dilution of the commercial solution with the phosphate buffers. Solutions of the analytes were prepared at the concentration of 0.1 mg/mL in a 10 mM disodium phosphate buffer (pH 7.0).

2.3. Apparatus

Electrophoretic experiments were performed by an HP^{3D}CE instrument from Agilent Technologies (Waldbronn, Germany). The data were collected on a personal computer, equipped with the software HPCE version A 09 (Agilent Technologies).

The separations were obtained at a constant voltage of 20 kV (anodic detection) with controlled temperature (30°C). The optimized partial filling conditions were as follows. Between the injections, the capillary was rinsed with aqueous phosphoric acid (100 mM) for 3 min by applying a constant pressure of 2 bar at the outlet end; rinses (3 min) with water and plain buffer (100 mM phosphate at pH 5.5), were then carried out at the pressure of 1 bar at the inlet end of the capillary. Finally, the capillary was partially filled with the chiral selector solution (240 μM of PGA in pH 5.5 phosphate buffer) at 50 mbar for 120 s at the inlet end. The CE sampling was hydrodynamically performed at 50 mbar for 3 s; the detection wavelength was 220 nm.

2.4. Coating procedure

The total length of the fused-silica capillary tubing was 48.5 cm; the on-column detection window was made by burning off the polyimide outer coating (about 0.3 cm) at 8.5 cm from the outlet end of the capillary. The capillary was then installed in the proper cartridge and the temperature was set at 30°C; the washing cycles were performed using sodium hydroxide 1.0 and 0.1 M, for 5 min each. An accurate rinsing procedure was then applied as follows: water, 0.1 M HCl, water and acetone (5 min each); then the capillary was filled with a 5% v/v solution of glycidiloxypropyltrimethoxysilane in chloroform and it was left at room temperature overnight. Acetone was flushed for 10 min in order to remove any traces of the silanizating reagent; a nitrogen flow for 10 min was finally applied to properly dry the inner surface of the activated capillary. The capillary tubing was then filled with aqueous pullulan solution (1% w/v) by applying a pressure of 2 bar, then it was introduced in oven at 120°C for 1 h to evaporate the water. The evaporation of water

left a dry layer of pullulan that resulted to be thermally adsorbed onto the inner surface. Afterward, the capillary was rinsed with acetone (5 min) and then filled with a 3% v/v solution of boron trifluoride diethyletherate (BF_3) in chloroform; under these conditions, the hydroxyl functions of the polysaccharide were chemically fixed to the epoxy groups of the activated surface by a BF_3 catalyzed reaction. After 1 h, a final rinse with acetone and water, in that order (5 min each), completed the procedure. The capillary was kept in a 100 mM solution of aqueous phosphoric acid during storage.

2.5. EOF mobility measurements

The measurement of the electroosmotic mobility at different pH conditions was performed using DMSO as the neutral marker in the short-end injection mode. Briefly, after conditioning of the capillary using the proper plain running buffer (sodium phosphate 100 mM at different pH values), the DMSO solution was sampled at the end of the capillary nearer to the detection window (effective length 8.5 cm) by a pressure of 25 mbar for 2 s. The applied voltage and capillary temperature were maintained at 10 kV and 30°C, respectively; the mean of three measurements for each of the tested buffers was plotted against the related pH value.

3. RESULTS AND DISCUSSION

In previous studies, PGA showed to be an effective chiral selector in HPLC stationary phases for the enantioresolution of a series of acidic compounds [24, 25]. Either microparticulate [23, 25] or monolithic supports [24] were used to immobilize PGA. In the present study, the potential of PGA as chiral selector was applied in free solution CE using the partial filling technique. As a first step in the development of a reliable enantioselective method, the interaction between the silanol groups of capillary wall and PGA had to be minimized. Subsequently, the effects of the experimental conditions (pH, PGA concentration, time of partial filling) on migration time and enantioresolution were evaluated.

3.1. Capillary coating

As shown in the first chapter, several types of coating procedures have been reported to be capable of hindering the adsorption of proteins to the capillary wall, either by permanent [27, 28] or dynamic procedures [29]. Solute–wall interactions are of relevant importance in the analysis of protein mixtures; in order to obtain separations with high theoretical plate numbers, these interactions have to be minimized. Furthermore, stronger antiadhesive properties of the inner capillary wall would be requested when proteins are used as chiral selectors in the BGE. In fact, by applying this approach, relatively high concentrations of proteins have to be dissolved in BGE; as a result of which, the risk of their adsorption onto the capillary wall and consequent blockage is more than likely. Dynamic coating often involves the use of additives to the BGE for the temporary modification of the silica properties; this approach has been successfully applied also in chiral CE using partial filling [13, 14]. However, the addition of modifiers could strongly affect the separation mechanism and enantiorecognition because of additional interactions additive – chiral selector occurring in the bulk solution [1–4, 10]. Differently, the use of a permanent coating seems to be a favorable choice to reduce the adsorption of proteins without effects on their ability as chiral additives to the BGE; under these conditions, the

enantiorecognition ability has to be ascribed only to the chiral selector. In preliminary experiments, relatively high concentrations of PGA were supplemented to the BGE in order to get enantioselectivity. In particular, conventional polyacrylamide-coated capillaries [30] were found to be unsuitable as they were blocked after very few injections. The same trouble was observed using commercially available PVA-coated capillaries. Therefore, a different permanent coating was developed according to the procedure proposed by Liao *et al.* [31] and Aguilar *et al.* [32], but using pullulan instead of cellulose derivatives as hydrophilic polymers. Pullulan is a neutral microbial polysaccharide that is produced in large quantities by fermentation; this biopolymer consists of maltotriose and maltotetraose units with both a-(1→4) and a-(1→6) linkages. This structure results in molecular flexibility and ability to form adhesive films suitable for coating of foods and pharmaceuticals [33].

These properties suggested pullulan as a suitable candidate for a static coating of the fused-silica capillary tubing. As the silanization step consisted in a well-known procedure [31, 32], in the present study, the optimization of the coating was focused on the binding of the polymer to the activated capillary surface. In particular, solutions of pullulan in the concentration range of 0.5–5.0% w/v were used. The characterization of the coating obtained under the different conditions, was performed by measurements of EOF mobility and by investigating its dependence on the pH in the range of 3.0–9.0 [28, 29, 34]. In Fig. 3.1, the plots of variation of EOF mobility under the influence of the buffer pH in differently treated capillaries (conventionally activated, silanized, and coated with pullulan 1%) are reported. For these measurements, the short-end injection mode was advantageously applied. Since in this approach, the effective length of the capillary is only 8.5 cm even in front of a very slow EOF mobility, the experiments can be carried out in a relatively short time. As shown in Fig. 3.1, the silanization step, significantly reduces the EOF mobility compared to the activated fused-silica capillary; however, a stronger suppression of EOF mobility was obtained after the coverage with pullulan. Interestingly, the use of 1% w/v pullulan aqueous solution resulted in the best EOF suppression; conversely

using higher concentration of pullulan, the EOF suppression was less effective. This behavior could be due to the high viscosity of concentrated pullulan solution and the consequent difficulty in controlling its homogeneous distribution into the capillary tubing. In general, the applied coating procedure, although involving multistep reactions, resulted to be simple and showed good reliability. Precisely, five capillaries were prepared successively according to the described process using aqueous pullulan 1% w/v; the EOF mobility was then measured as described above, in a pH 5.0 phosphate buffer (100 mM) and the mean migration time of the neutral marker DMSO was 33.5 min (RSD% = 5.2).

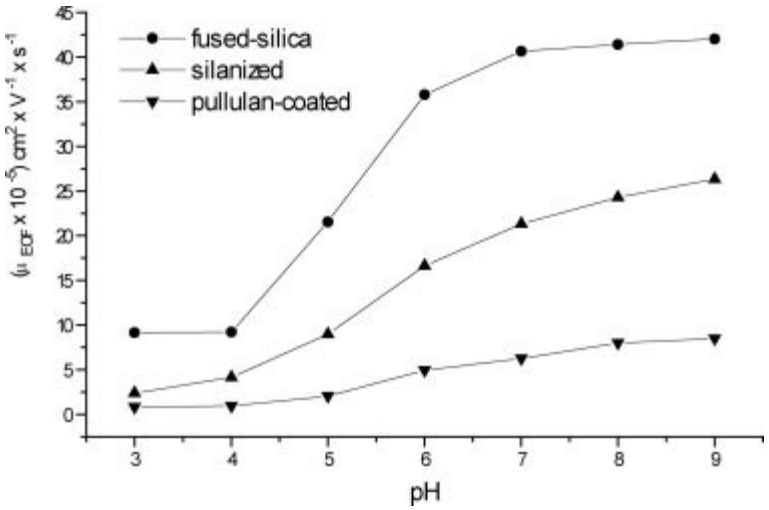

Fig. 3.1. Effect of running buffer pH on the electroosmotic mobility of capillaries subjected to different treatments: fused-silica capillary activated by washing, in the order, with sodium hydroxide 1.0, 0.1 M, and water for 10 min each (●); silanized capillary with glycidoxypropyltrimethoxysilane (▲); 1% pullulan-coated capillary (▼). BGE: sodium phosphate running buffer (100 mM). CE conditions: capillary length (48.5 cm total length; 8.5 cm effective length) with id of 50 μm; voltage 10 kV; hydrodynamic injection of DMSO aqueous solution (EOF marker) at 25 mbar for 2 s. Temperature, 307C; detection at 200 nm.

3.2. Enantioseparations using PGA as chiral selector

After the development of the suitable capillary coating, the goal of the work was the application of PGA as chiral selector in free solution CE. In previous studies conducted with HPLC, the class of profens was assumed as the model in evaluating the performance of PGA-CSPs [23, 25]. Similarly, in the present investigation,

rac-ketoprofen was considered as the analyte for the optimization of the partial filling technique. In chiral CE, the enantioseparation is controlled by the difference in binding constants of the enantiomers to the chiral selector; however, a significant role is also played by the differences between mobility of complexed and free solute [3, 4, 12, 34]. In particular, using the partial filling technique, the availability of a system with suppressed EOF can allow the opposite migration direction of protein and solutes, thus favoring the enantioseparation [2–12]. Since the p*I* of PGA from *E. coli* is reported to be 5.9 [36] and the p*K*a of ketoprofen is 4.6 [37], the most favorable conditions in obtaining enantioresolution are achieved using running buffers in a restricted pH range; thus, this parameter has to be carefully considered.

3.2.1 Effect of the buffer pH on the enantioresolution and migration time of *rac*-ketoprofen

The considerations given above were confirmed by the experimental evaluation of enantioseparation of *rac*-ketoprofen using a phosphate buffer (100 mM) containing 240 mM PGA in a pH range from 4.5–7.5 and by partial filling of the capillary for 120 s at 50 mbar. As the pullulan based coating suppressed the EOF, a voltage of 20 kV in negative polarity mode (anodic detection) was applied for the detection of the anionic ketoprofen.

In Figs. 3.2a and b, the variation of enantioresolution and migration time of the enantiomers of ketoprofen at different buffer pHs are shown, respectively; the highest enantioseparation was kept at pH 5.5. The enantioselectivity is maximized by increasing the mobility difference between the complexed (μp) and the free solute (μs); this favourable condition is achieved at pH 5.5 where PGA resulted predominantly in its cationic form (p*I* = 5.9), whereas an adequate dissociation of *rac*-ketoprofen is still obtained. These conditions realized the typical countercurrent separation mode; at pH values higher than 5.5, the reduced positive charge of PGA decreased the difference (μs - μp) and, at the same time, weaker electrostatic interactions were involved between PGA and ketoprofen. According to this

hypothesis, the anionic mobility of the ketoprofen enantiomers was found to progressively increase by increasing the pH values. Conversely, at pH values lower than 5.5, the anionic character of the solute is decreased as shown by its increased migration time (Fig. 3.2b); the consequent weakness of the interactions with the PGA can explain the decreased enantioresolution. For these reasons, pH 5.5 was selected as optimum for the further experiments.

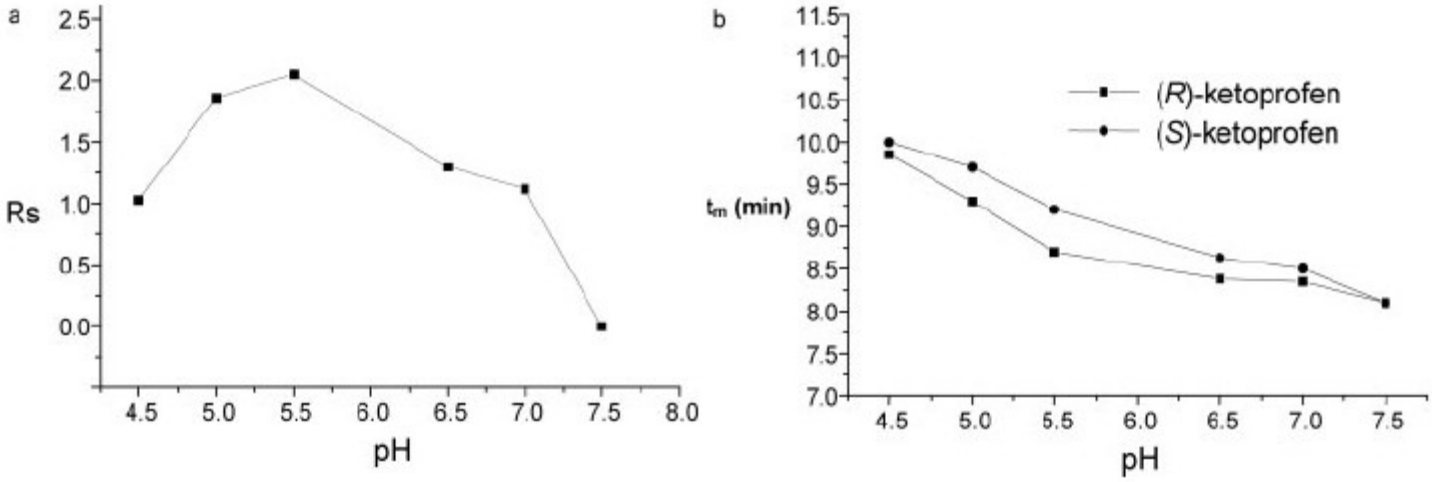

Fig. 3.2. Effect of running buffer pH on the enantioresolution of *rac*-ketoprofen (3.2a) and on the migration time of the single enantiomers of ketoprofen (3.2b), in partial filling CE using PGA as a chiral selector in a pullulan-coated capillary. Conditions: 1% pullulan-coated capillary of 40 cm effective length (total length 48.5 cm) with id of 50 μm. BGE: 100 mM sodium phosphate at different pH values, supplemented with PGA at a final concentration of 240 μM. Partial filling performed at 50 mbar for 120 s; voltage of 20 kV (anodic detection); temperature, 30°C. Hydrodynamic injection of *rac*-ketoprofen (0.1 mg/mL) at 50 mbar for 3 s.

3.2.2. Effect of plug length of PGA on enantioresolution of *rac*-ketoprofen

In partial filling CE, the length of the chiral selector zone introduced into the capillary could be thought as the length of a chiral column in LC; thus, this parameter strongly affects the enantioresolution and it has to be carefully selected. The requirement for the detection of the enantiomers without interference by the chiral selector, is the limiting factor in this step of optimization. A PGA solution (240 μM) at pH 5.5 was introduced into the capillary by pressure of 50 mbar; the time of loading was varied, in different experiments, from 60 to 140 s in order to obtain progressively increased chiral selector plug lengths. Under the investigated conditions, *rac*-ketoprofen was analyzed and, as expected, the obtained enantioresolution values were found to increase with the increase in the plug length. However, loading time higher than 120 s was not useful because of a slow but progressive baseline drift that interfered with the detection of the analytes.

The effective length (to detector) of the used capillary was 40 cm, and the working

PGA solution (240 μM, pH 5.5) was charged by supplying a pressure of 50 mbar; under these conditions, the front of the PGA zone reached the optical window after 360 s, thus the optimum plug length (120 s) was correspondent to about 33% of the effective capillary length.

3.2.3. Effect of PGA concentration on enantioresolution of *rac*-ketoprofen

Pullulan is endowed with its own chiral nature that was previously exploited by using it as an additive dissolved into the electrophoretic BGE for the enantioresolution of basic racemates [38]. From these considerations, the pullulan layer used as an hydrophilic coating in the present study, could provide the capillary with an enantiorecognition ability in the open-tubular CEC mode (OTCEC). However, in general, the limited phase ratio and low separation capability are the main disadvantages of the OTCEC approach [39–41]; actually, as observed in the present investigation, the presence of PGA as additive to the BGE, was found to be essential to obtain chiral separation. In Fig. 3.3, the influence of PGA concentration (range 60–370 μM) on the enantioresolution of *rac*-ketoprofen using a 100 mM phosphate buffer pH 5.5 under partial filling conditions of 120 s is shown. For PGA concentrations below 60 μM, a comigration of the enantiomers was observed. Increasing PGA concentrations provided a progressive improvement of enantioresolution; however, above 240 μM, a baseline drift reduced the detectability of the analyte similar to the effect previously observed under conditions of long loading time. This behavior could be ascribed, in both the cases, to the presence of PGA impurities possessing anionic mobility and thus migrating toward the detection window; this drawback suggested the use of a pure and fresh enzyme. The optimum conditions for the further experiments were as following: 100 mM phosphate buffer (pH 5.5) containing 240 μM PGA using a partial filling of 120 s at 50 mbar at a constant temperature of 30°C and voltage of 20 kV. The detection was performed at 220 nm and the samples were hydrodynamically injected for 3 s at 50 mbar.

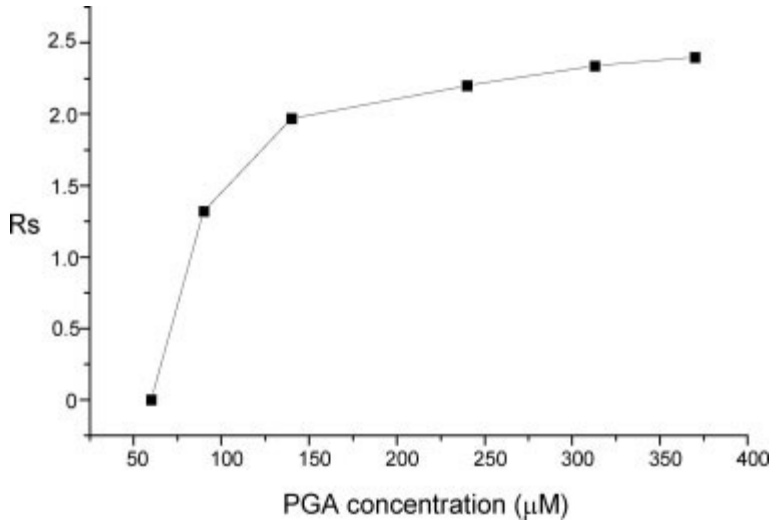

Fig. 3.3. Effect of PGA concentration on the enantioresolution of *rac*-ketoprofen. Conditions same as in Fig. 3.2 using 100 mM sodium phosphate BGE (pH 5.5) supplemented with PGA at different concentrations.

3.2.4 Enantioseparation of different racemates

The electrophoretic conditions, optimized for the enantioseparation of *rac*-ketoprofen, were applied to the analysis of a series of acidic compounds, most of them of pharmaceutical interest such as the anti-inflammatory drugs of the class of profens. As shown in Fig. 3.4, for some of the tested racemates, the enantioseparation and/or the peak shape was not optimal because general electrophoretic conditions

were applied without a specific optimization; nevertheless, good versatility of the proposed enantioselective method can be observed. Furthermore, the availability of single enantiomers of some of the studied compounds allowed the migration order to be determined. The (*S*)-enantiomer of ketoprofen was the second migrating peak, conversely, for flurbiprofen, 2-(4-chlorophenoxy)-phenylacetic acid, and for 2-(4-chlorophenoxy)-phenylpropionic acid, the (*S*)-enantiomer was the first migrating peak (Fig. 3.4). In particular, for 2-(4-chlorophenoxy)-phenylacetic acid and 2-(4-chlorophenoxy)-phenylpropionic acid, this behavior confirmed the evidences of HPLC studies [25] where the elution order *S/R* was demonstrated. This result, obtained using PGA in free solution, suggests that the immobilization procedure used in the development of PGA-CSPs did not alter the enantioselective properties of the enzyme.

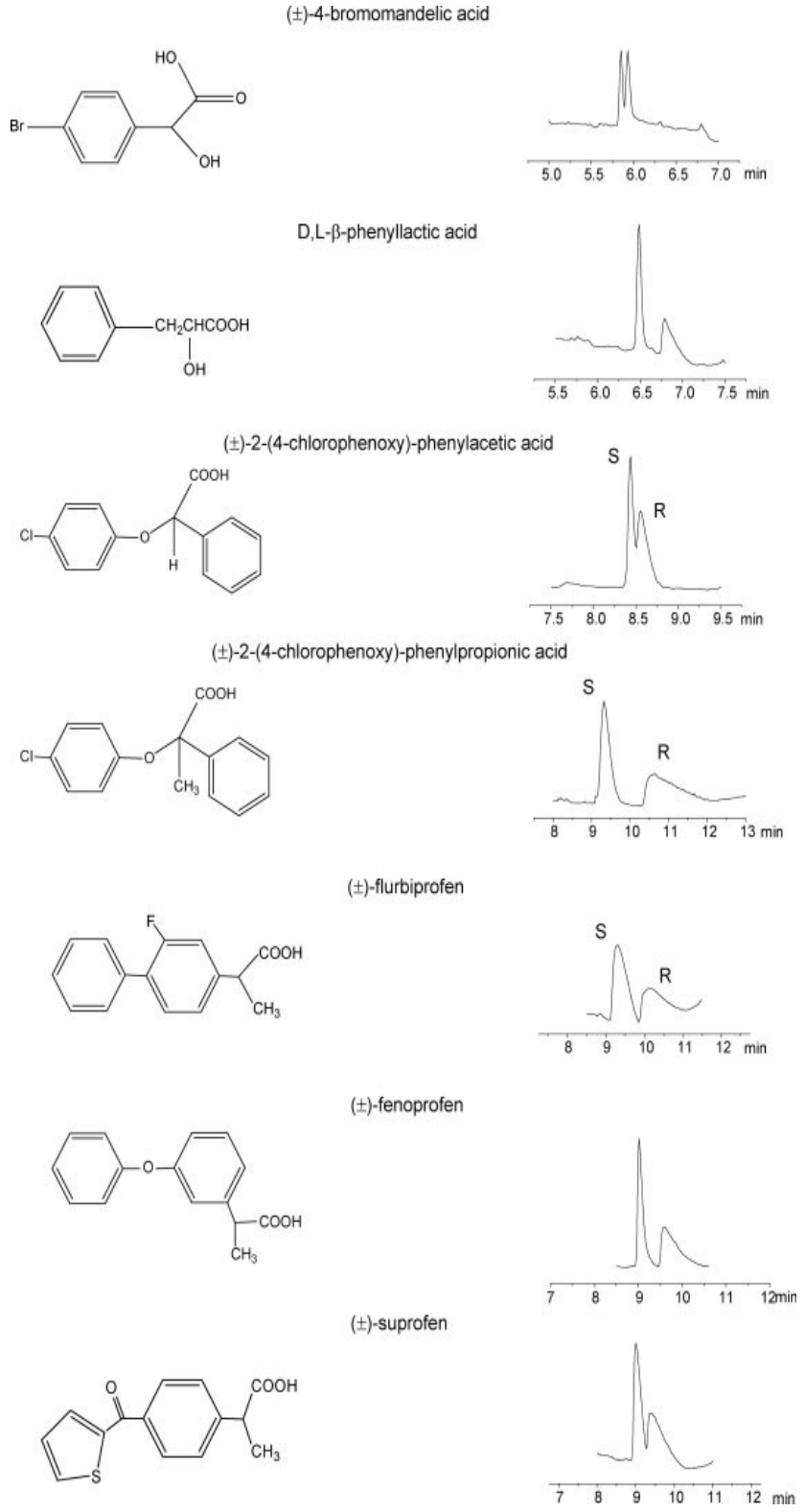

Figure 3.4. Structures and CE enantioseparations of the studied chiral acidic compounds using PGA as the chiral selector in partial filling conditions. The migration order (*S*/*R*), was indicated only for the compounds for which one single enantiomer was available. Conditions were the same as in Fig. 3 using a 100 mM sodium phosphate BGE (pH 5.5) supplemented with PGA at 240 μM. Hydrodynamic injection of the analytes (0.1 mg/mL) at 50 mbar for 3 s.

3.3. Analytical parameters

The reliability of the proposed procedure was demonstrated by data of reproducibility of migration time and enantioresolution of the studied racemates. The results of these determinations are reported in Table 3.1; as shown, good RSD% values were obtained. Furthermore, in order to prove the ability of the proposed method in accurate quantitation of enantiomers, the determination of the ratio of an undesired enantiomer to the main enantiomer was carried out. More precisely, ketoprofen was chosen as the test analyte because of its interest as a widespread drug, as well as for the good enantioresolution value obtained in the applied CE conditions and also due to the availability of the pure (*S*)-enantiomer. *rac*-Ketoprofen and (*S*)-ketoprofen solutions were mixed in order to obtain a final concentration of 62.5 μg/mL of (*S*)-enantiomer (the main enantiomer) in the presence of (*R*)-ketoprofen at the enantiomeric ratio of 1.20% w/w. In Fig. 3.5, the chiral separation of this mixture is shown using UV detection at 200 nm; by measuring the obtained corrected peak area, the enantiomeric ratio for (*R*)-ketoprofen was found to be 1.16% (RSD 5.2%; $n = 4$). These preliminary results suggested the reliability of the proposed method for quantitative chiral analysis also at impurity level.

Table 3.1. Reproducibility of migration times and enantioresolution of the studied racemates using the optimized chiral conditions

Analyte	t_mI (RSD%; $n = 6$)[a]	t_mII (RSD %; $n = 6$)[a]	R_s (RSD %; $n = 6$)[a]
(±)-Ketoprofen	8.75 (1.40; 3.16[b])	9.18 (1.54; 3.23[b])	2.1 (1.80; 2.52[b])
(±)-4-Bromomandelic acid	5.72 (1.0)	5.85 (1.8)	1.2 (2.1)
DL-Phenyllactic acid	6.50 (0.7)	6.71 (1.2)	2.0 (3.5)
(±)-2-(4-Chlorophenoxy)-phenylacetic acid	8.43 (1.2)	8.52 (1.6)	0.9 (3.1)
(±)-2-(4-Chlorophenoxy)-phenylpropionic acid	9.36 (2.7)	10.52 (2.0)	2.3 (2.2)
(±)-Flurbiprofen	9.48 (1.1)	10.12 (1.5)	1.0 (2.5)
(±)-Fenoprofen	8.95 (1.0)	9.60 (0.8)	1.5 (4.8)
(±)-Suprofen	8.94 (0.9)	9.24 (1.2)	1.3 (4.1)

a) Intraday values.
b) Interday values (RSD %; $n = 18$).
t_mI and t_mII are the mean migration times of the first and second migrating enantiomer.

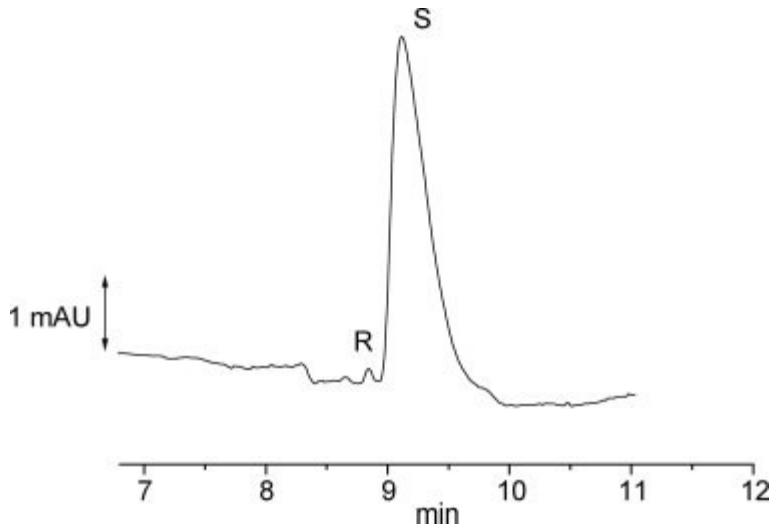

Fig. 3.5. Electropherogram of (*S*)-ketoprofen containing 1.20% w/w of the (*R*)-enantiomer. Detection at 200 nm; other conditions same as in Fig. 3.4.

3.4. Test of stability of the pullulan coating

The stability of the pullulan coating was tested by exposing the capillary to an aqueous 0.1 M sodium carbonate buffer (pH 9.6) overnight; the coating did not show any indication of deterioration in the subsequent electrophoretic chiral analysis of *rac*-ketoprofen. Finally, the longterm stability of the capillary coating was investigated by consecutive runs performed with *rac*-ketoprofen under the optimum partial filling conditions. The electropherograms of Fig. 3.6 show that after 100 injections, the performance of the capillary is practically unchanged and the shift in migration time as well as in enantioresolution, is negligible.

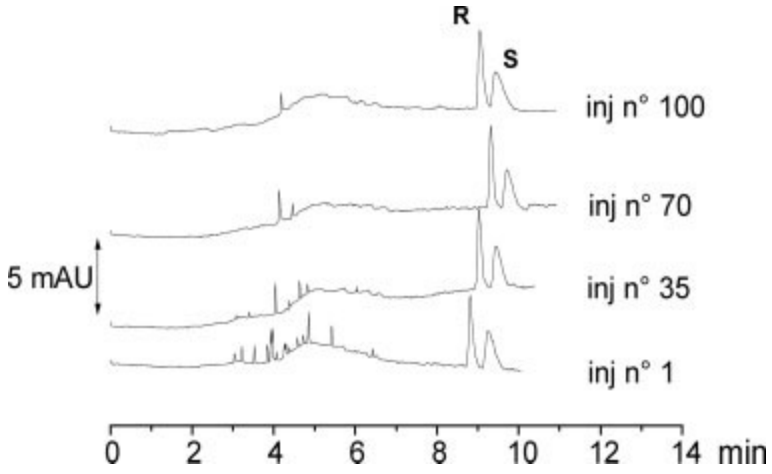

Fig. 3.6. Long-term stability of the capillary coating. The electropherograms of the chiral separation of *rac*ketoprofen in the optimized partial filling conditions (as in Fig. 3.4) were consecutively obtained in the same capillary.

4. Conclusion

The enzyme PGA was used for the first time as a suitable chiral selector in partial filling CE; this approach required a coated capillary to be used in order to reduce the interactions of the protein with the silica surface of the inner capillary wall. In the present study, pullulan was used as the hydrophilic polymer with successful results; high EOF suppression, reproducibility of the migration time, alkaline and long-term stability, confirmed efficiency in silanol shielding of the proposed coating. The EOF suppression obtained in coated capillaries allowed an easy fulfillment of the typical countercurrent mode of partial filling CE, where the analyte and chiral selector migrate in opposite directions, realizing the best condition for high enantioresolution. In the developed partial filling conditions, a general good enantioselectivity of PGA was achieved for a series of acidic compounds; regarding ketoprofen, the opportunity for enantiomeric ratio quantitation at impurity level was also shown. These results confirmed those obtained previously using PGA as an immobilized CSP in HPLC analysis.

References

[1] D.K. Lloyd, S. Li, P. Ryan, J. Chromatogr. A 694 (1995) 285.

[2] D.K. Lloyd, A-F. Aubry, E. De Lorenzi, J. Chromatogr. A 792 (1997) 349.

[3] J. Haginaka, J. Chromatogr. A 875 (2000) 235.

[4] Y. Tanaka, S. Terabe, J. Biochem. Biophys. Methods 48 (2001) 103.

[5] L. Valtcheva, J. Mohammad, G. Pettersson, S. Hjertén, J. Chromatogr. 638 (1993) 263.

[6] A. Amini, U. Paulsen-Sorman, D. Westerlund, Chromatographia 50 (1999) 497.

[7] S. Fanali, C. Desiderio, J. High Resolut. Chromatogr. 19 (1996) 322.

[8] E. De Lorenzi, G. Massolini, M. Quaglia, C. Galbusera, G. Caccialanza, Electrophoresis 20 (1999) 2739.

[9] M. Hedeland, R. Isaksson, C. Pettersson, J. Chromatogr. A 807 (1998) 297.

[10] M. Chiari, M. Cretich, V. Desperati, C. Marinzi, et al., Electrophoresis 21 (2000) 2343.

[11] H. Katayama, Y. Ishihama, N. Asakawa, J. Chromatogr. A 875 (2000) 315.

[12] M. Hedeland, M. Nygård, R. Isaksson, C. Pettersson, Electrophoresis 21 (2000) 1587.

[13] J. Kang, D. Wistuba, V. Schurig, Electrophoresis 24 (2003) 2674.

[14] Z. Jiang, J. Kang, D. Bischoff, B. Bister, et al., Electrophoresis 25 (2004) 2687.

[15] J.J. Martinez-Pla, Y. Martín-Biosca, S. Sagrado, R.M. Villanueva-Camañas, M.J. Medina-Hernández, J. Chromatogr. A 1048 (2004) 111.

[16] M.A. Martinez-Gomez, R.M. Villanueva-Camañas, S. Sagrado, M.J. Medina-Hernández, Electrophoresis 26 (2005) 4116.

[17] S. Grard, Ph. Morin, M. Dreux, J.P. Ribet, J. Chromatogr. A 926 (2001) 3.

[18] Y. Tanaka, Y. Kishimoto, S. Terabe, J. Chromatogr. A 802 (1998) 83.

[19] Y. Tanaka, K. Otsuka, S. Terabe, J. Chromatogr. A 875 (2000) 323.

[20] R. Gotti, E. Calleri, G. Massolini, S. Furlanetto, V. Cavrini, Electrophoresis 27 (2006) 4746.

[21] M. Arroyo, I. de la Mata, C. Acebal, M.P. Castillon, App. Microbiol. Biotechnol.

60 (2003) 507.
[22] E. Calleri, C. Temporini, G. Massolini, G. Caccialanza, J. Pharm. Biomed. Anal. 35 (2004) 243.
[23] G. Massolini, E. Calleri, E. De Lorenzi, M. Pregnolato, et al., J. Chromatogr. A 921 (2001) 147.
[24] E. Calleri, G. Massolini, D. Lubda, C. Temporini, et al., J. Chromatogr. A 1031 (2004) 93.
[25] E. Calleri, G. Massolini, F. Loiodice, G. Fracchiolla, et al., J.Chromatogr. A 958 (2002) 131.
[26] G. Massolini, E. Calleri, A. Lavecchia, F. Loiodice, et al., Anal. Chem. 75 (2003), 535.
[27] C-Y Liu, Electrophoresis 22 (2001) 612.
[28] J. Horváth, V. Dolník, Electrophoresis 22 (2001) 644.
[29] P.G. Righetti, C. Gelfi, B. Verzola, L. Castelletti, Electrophoresis 22 (2001) 603.
[30] S. Hjertén, J. Chromatogr. 347 (1985) 191.
[31] J-L. Liao, J. Abramson, S. Hjertén, J. Capil. Electrophor. 4 (1995) 191.
[32] C. Aguilar, A.J.P. Hofte, U.R. Tjaden, J. van der Greef, J.Chromatogr. A 926 (2001) 57.
[33] J.W. Lee, W.G. Yeomans, A.L. Allen, F. Deng, et al., Appl.Environ. Microbiol. 65 (1999) 5265.
[34] J. Kohr, H. Engelhardt, J. Chromatogr. 652 (1993) 309.
[35] B. Chankvetadze, Chem. Soc. Rev. 33 (2004) 337.
[36] A. Bossi, M. Cretich, P.G. Righetti, Biotechnol. Bioeng. 60 (1998) 454.
[37] C. Hansch, P.G. Sammes, J.B. Taylor, in: Drayton, C. J. (Ed.), Comprehensive Medicinal Chemistry, Pergamon Press, New York 1990, Vol. 6.
[38] R. Gotti, R. Pomponio, V. Cavrini, Chromatographia 52 (2000) 273.
[39] Z. Liu, K. Otsuka, S. Terabe, M. Motokawa, N. Tanaka, Electrophoresis 23 (2002) 2973.
[40] J.J. Pesek, M.T. Matyska, J. Chromatogr. A 887 (2000) 31.

[41] Z. Liu, K. Otsuka, S. Terabe, J. Chromatogr. A 961 (2002) 285.

Chapter 4 :

Analysis of human histone H4 by capillary electrophoresis in a pullulan-coated capillary, LC-ESI-MS and MALDI-TOF MS.

1. INTRODUCTION

The analysis of the human histone H4 (a core histone) is in general very important, in particular it gains specific significance in estimating the activity of a series of enzymes such as histone deacetylase (HDAC) and histone acetyltransferase (HAT). These enzymes are involved in the post-translational acetylation of the n-terminal domains of histones thus influencing gene transcription through the modulation of nucleosomal packaging of DNA.

The nucleosome is the basic structural unit of eukariotic chromosomes and consists of a DNA molecule associated with a histone octamer which comprises pairs of the core histones H2A, H2B, H3, and H4. The nucleosomes are joined by linker DNA and histone H1 to form chromatin. It is well established that histones play an important role in DNA transcription, replication, repair, and recombination (Fig. 4.1). The N-terminal domains of histones, commonly termed "tails", protrude from the nucleosome and are subjected to several types of covalent modification, such as acetylation, methylation, phosphorylation, ADP-ribosilation, and ubiquitination. These post-translational modifications of specific residues in the tails of core histones have been demonstrated to be critical to their regulatory function. In particular, acetylation is a very specific covalent modification producing various forms that play distinct functional roles, and is generally correlated with transcriptionally active or silent chromatin [1].

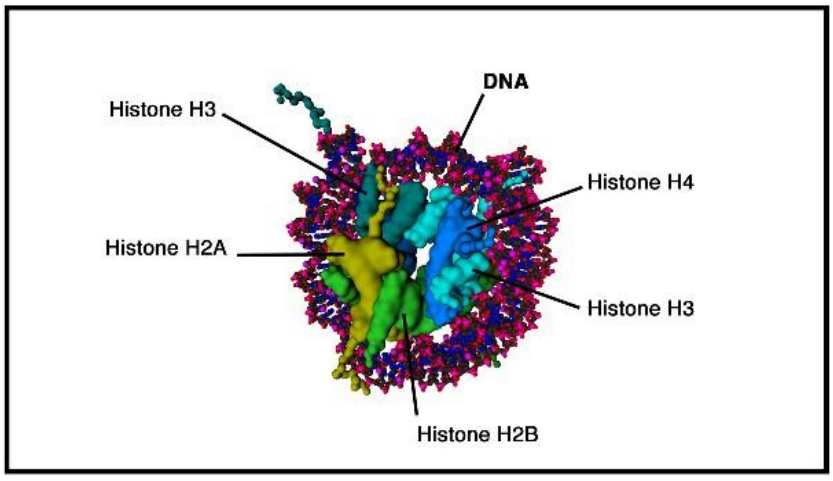

Fig. 4.1. "Core" Histones

The acetylation status of core histones plays a pivotal role in regulating gene transcription through the modulation of nucleosomal packaging of DNA. In a hypoacetylated state, nucleosomes are tightly compacted; the protonated primary amine groups of lysines establish ionic interactions with the phosphate groups of DNA nucleotides, resulting in a transcriptional repression due to restricted access of transcription factors to their target DNA. Conversely, histone acetylation leads to relaxed nucleosomal structures, giving rise to a transcriptionally permissive chromatin state. As previously said HDAC and HAT affect the levels of histone acetylation. (Fig. 4.2) In recent years, an increasing interest in HDACs as a target for new antineoplastic drugs has been registered due to the ability of HDAC inhibitors to arrest tumour cell growth *in vitro* and in animal models at doses that cause little or no toxicity [2,3].

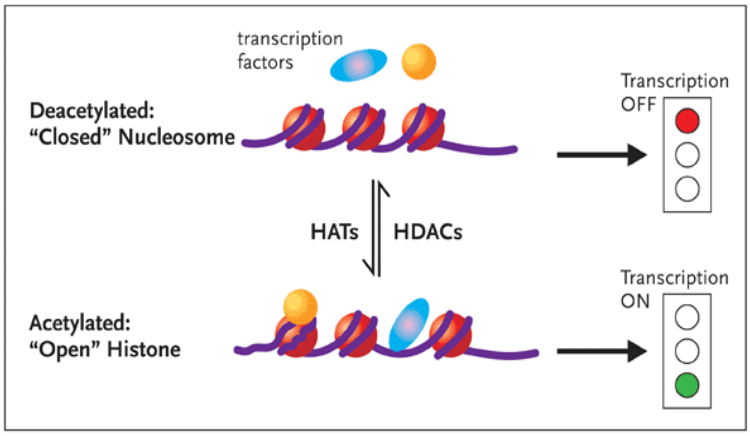

Fig. 4.2. Histones acetylation and its role on gene transcription.

HDAC inhibitors (short chain compounds, such as butyrate and valproate, and hydroxamic acids such as thrichostatin A) have been described as potential anticancer drugs in a variety of preclinical studies [4]. In fact, treatment of cells with these inhibitors results in the increase of highly acetylated forms of histones, which affect gene expression, cell differentiation, and apoptosis. The evaluation of the state of histone acetylation is very important due to evaluate the activity of HDAC inhibitors. The separation of histones is difficult because of the combination of their high molecular mass (strong adsorption to the capillary wall via Van der Waals-

hydrophobic interactions) and high p*I* values (p*I* > 9).

An interesting approach to prevent the adsorption to the silica wall was proprosed by Lindner *et al*. [5, 6]. In this system HPMC was used as an additive for the dynamic coating in preventing the adsorption of histone to the capillary wall. The reliability of the proposed CE system was also proved by recent applications related to the evaluation of histone modifications in cancer cells [7, 8]. However, further advances in this field are going to be expected; in fact in recent years the necessity to estimate the efficiency of inhibitors of HAT and HDAC is carried out by monitoring the variation of the acetylation profile of the histones [2,3]. With the interest in clarifying the effectiveness of HATs and HDACs inhibitors as anticancer drugs, in the present study the analysis of the acetylated isoforms of histone H4 has been carried out by the integrated use of CE, LC-ESI-MS and MALDI-TOF MS. In particular, the pullulan-coated CE capillary [9], we firstly tested in the analysis of standard basic proteins (cytochrome c, trypsinogen, α-chymotrypsinogen A and lysozyme), was then applied, for the first time, in the separation of the acetylated isoforms of histones H4 from HT29 cell lines in order to monitor the acetylation level after treatment of the cell lines with histone deacetylase inhibitors (HDACs) [10]

2. EXPERIMENTAL

2.1. Materials

Fused-silica capillaries (50 μm id, 48.5 cm total length, 40 cm length to the detector) were from Composite Metal Service (Ilkley, UK). Pullulan from *Aeurobasidium pullulans*, cytochrome *c* from bovine heart, trypsinogen and α-chymotrypsinogen A both from bovine pancreas, lysozyme from egg white albumin, dimethylsulfoxide (DMSO), triethanolamine and heptafluorobutyric acid (HFBA) were provided by Sigma-Aldrich (Milan, Italy). (3-Glycidiloxypropyl)trimethoxysilane, boron trifluoride diethyl etherate (BF_3) and (hydroxypropyl)methyl cellulose at the viscosity of 4000 cps (HPMC), were from Fluka (Buchs, Switzerland). Experiments on the inhibition of histone deacetylase were performed using sodium butyrate (Sigma-Aldrich), and 9-hydroxystearic acid (9 HSA) (synthesized in our laboratory).

Phosphoric acid, hydrochloric acid, sodium hydroxide, tris (hydroxymethyl)-aminomethane (Tris), and all the other chemicals of analytical grade, were purchased from Carlo Erba Reagenti (Milan, Italy). Water used for the preparation of solutions and running buffers, was purified by a Milli-RX apparatus (Millipore, Milford, MA, USA).

2.2. Solutions

Tris-phosphate buffer used as the background electrolyte (BGE) in the analysis of basic proteins was prepared at different concentrations in water and the pH was adjusted at the desired value using a 0.1 M aqueous solution of phosphoric acid. Triethanolamine-phosphate buffer used as the BGE in analysis of histone H4 was prepared at the concentration of 100 mM in water and the pH was adjusted to 2.5 with 0.1 M phosphoric acid solution. An aqueous solution of DMSO (0.01 % w/v) was used as the marker of EOF. A mixture of the standard basic proteins (cytochrome *c*, trypsinogen, α-chymotrypsinogen A and lysozyme), each at the concentration of 25 μg/mL, was prepared in water and used as a test sample.

2.3. Apparatus

Electrophoretic experiments were performed by a HP^{3D}CE instrument from Agilent Technologies (Waldbronn, Germany). The data were collected on a personal computer equipped with the software HPCE version A 09 (Agilent Technologies).

The separations of the standard basic proteins were obtained at a constant voltage of 20 kV, at the controlled temperature of 30°C. The analysis of histones H4 was carried out at a voltage of 10 kV and temperature of 40°C. In order to obtain reproducible migration times, the capillary was rinsed between runs with the separation buffer for 1 min, applying a constant pressure of 5 bar at the outlet end, and then with the separation buffer again for 1 min applying a constant pressure of 5 bar at the inlet end. The CE sampling was hydrodynamically performed at 50 mbar for 3 s; the UV detection wavelength was set at 200 nm.

2.4. Coating procedure

A fused-silica capillary tubing (48.5 cm of total length and 40 cm of effective length) was subjected to the coating procedure with the polysaccharide pullulan according to the method described in Chapter 3 (section 2.4) [9]. A stable chemically bonded coverage was obtained and the coated capillary was kept in a 100 mM aqueous solution of phosphoric acid during storage.

2.5. Histones extraction and fractionation

Histone proteins were extracted from nuclei of HT29 cells; in particular, the cells were treated for six hours with histone deacetylase inhibitors (5 mM sodium butyrate or 100 μM 9 HSA) and the histone fraction was immediately extracted. Similarly, untreated cells were used as control. Finally, by following a previously reported procedure [11], samples of 1 mg/mL concentration in water (50 – 100 μM) were obtained.

LC preparative separations of the histone proteins were performed using a Jasco PU-1585 liquid chromatograph (Jasco Corporation, Tokio, Japan) with a Rheodyne 7281

injection valve (20µL sample loop) interfaced with UV detector (Jasco, UV 1575), fixed at 215 nm.

Reversed phase chromatographic separation of histone H4 were performed on a C_4 Jupiter column, (4.6 x 150 mm I.D., 5µm, 300 Å, Phenomenex, Torrance, CA, USA), assembled with a SecurityGuard™ HPLC system consisting of a C18 guard cartridge (4.0 x 3.0 mm I.D., Phenomenex) inserted into its cartridge holder, using a gradient elution from A [water: HFBA (100:0.06) (v/v)]/ B [acetonitrile: HFBA (100:0.06) (v/v)] 62/38 (v/v), to A/B 30/70 (v/v), in 90 min., at a flow rate of 0.4 mL/min. The column was equilibrated with the mobile phase composition of the starting condition for 10 min before the next injection.

Repeated injections of histone samples were performed and histone H4 was eluted from the column, collected and dried under vacuum. The purity of the isolated protein was checked under the same chromatographic conditions.

2.6. HPLC-ESI-MS analysis of histone H4

LC-MS analyses of extracted histone proteins from control and treated HT29 cells were performed using a Jasco PU-1585 liquid chromatograph (Jasco Corporation, Tokio, Japan) with a Rheodyne 7281 injection valve (10µL sample loop) interfaced with the LCQ-Duo mass detector (ThermoFinnigan), equipped with an electrospray ionisation (ESI) source. The ESI system employed a 4.5 kV spray voltage (positive polarity), a capillary temperature of 170°C and a cone voltage of 46 V. The mass chromatograms were recorded in total ion current (TIC), made within 500 and 2,000 *m/z*.

Deconvoluted ESI mass spectra of histones were obtained by using Mag Tran 1.0 software. The peak averaged mass spectra were reconstructed and the mass of the histones and their isoforms, calculated. The relative abundance of each histone isoform was derived and transformed into relative percent amount.

2.7. Digestion of histone H4 with endoproteinase Arg-C and MALDI-TOF MS analysis

An aliquot of 10 μL of histone H4 (10mM) was digested with endoproteinase Arg-C (Roche) in 20 mM NH_4HCO_3 at enzyme ratio 1:25 at 37°C for 18h.

MALDI-TOF MS analysis of the Arg-C digested histone H4 was performed using a Voyager DE Pro (Applied Biosystems, Foster City, CA) equipped with a pulsed N_2 laser operating at 337 nm. Positive ion spectra were acquired in reflector mode over an m/z range of 500-5,000 amu, using a 20,000 V accelerating voltage, a 14,900 V grid voltage and an extraction delay time of 150 ns. The spectrum of each spot was obtained by averaging the results of 100 laser shots.

Histone H4 digest spectra were internally calibrated on 40-45 and 1-17 theoretical histone digest peptide masses that were sufficiently abundant in the spectra.

The matrix was a solution of 10 mg/mL α-Cyano-4-hydroxycinnamic acid (CHCA) in 1:1 acetonitrile/water containing 0.5% formic acid. The analysis was performed by spotting 1 μL of the sample mixed with an equal volume of the matrix solution onto the target plate.

3. RESULTS AND DISCUSSION

The main objective of the present study was the development of a reliable and efficient CZE method for the separation of acetylated histone H4 isoforms. In order to accomplish this task the use of a pullulan-coated capillary was approached to prevent the adsorption of these highly basic proteins to the silica capillary wall. Therefore the work involved two steps: a) suitability of the coated capillary for the separation of basic proteins; b) separation of the acetylated histone H4 isoforms.

3.1. Separation of basic proteins in pullulan coated capillary

As shown in the previous chapter pullulan, was successfully used to develop a covalently bonded layer to the inner silica surface of CE capillaries useful in protein-based chiral separations [9]. The separation of basic proteins in CZE represents a difficult task because on an uncoated capillary, a severe peak tailing is always displayed due to the electrostatic attraction between the cationic proteins and the negatively charged silica surface. It is become right common to test the performances of capillary coating by trying the separation of a mixture of standard basic proteins. To this regard, cytochrome *c*, trypsinogen, α-chymotrypsinogen A and lysozyme are widely chosen because they are easily affordable and constitute a representative model of basic proteins (isoelectric point p*I* ranged between 9.3 – 11.0, and molecular masses within 12.5 – 25.0 kDa) [12 – 17]; thus using this kind of standard mixtures, comparison of the performances of different coatings is easily carried out. An aqueous solution of the standard proteins (each at 25 μg/mL) was analysed under general acidic (Tris-phosphate pH 2.5 BGE) CZE conditions and the effect of buffer concentration on the efficiency (theoretical plates number) of each of the studied proteins was evaluated in the range within 50 – 200 mM. The best compromise on the performance of the four proteins was achieved using a 100 mM Tris-phosphate buffer (pH 2.5); under these conditions, electropherograms of the separation of the studied proteins in pullulan-coated capillary are shown in Fig. 4.3a. Under the same electrophoretic conditions the protein mixture was also analysed in an uncoated

fused-silica capillary; as shown in Fig. 4.3b, a strong reduction of efficiency was observed and only three peaks were recovered with a significant loss in sensitivity for each of them. Improvements of the separation could be achieved in a fused silica capillary by supplementing the BGE with a 0.015 % (w/v) of HPMC (Fig. 4.3c); higher concentration of HPMC did not improve the electrophoretic performance and a general lower recovery for each of the analytes (in particular cytochrome *c*) was observed in comparison to the results obtained using a pullulan-coated capillary. Furthermore, in our application, the pullulan-coated capillary showed superior performances in efficiency, resolution and analysis time also in comparison to the HPMC-coated capillary previously applied in CE analysis of standard basic proteins and histones [17, 18]. In Table 4.1 the repeatability of the migration time and the corrected peak area as well as the efficiency, expressed as the theoretical plates number for each of the proteins analysed using pullulan-coated capillary, are reported. Excellent RSD % values (intraday, n = 5) were found, confirming the possibility to apply the proposed coating for analysis of unknown samples. Regarding the long-term stability of the coating, it has been proved that significant deterioration of RSD % of migration times and corrected peak area of the studied proteins were not observed at least up to 100 injections [10].

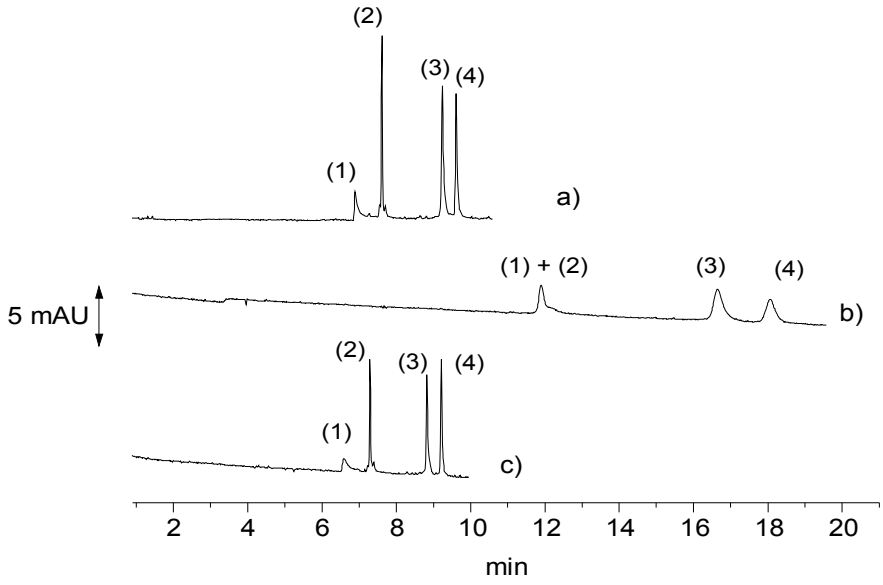

Fig. 4.3. Electropherograms of basic proteins (each at 25 μg/mL, aqueous solution) in different capillaries: (a) pullulan-coated; (b) fused-silica; (c) fused-silica with dynamic coating*.

CE conditions: capillary of 48.5 cm total length (40 cm effective length; i.d. 50 μm); BGE constituted of a pH 2.5 Tris-phosphate (100 mM); voltage at 20 kV; temperature at 30 °C; hydrodynamic injection at 50 mbar x 3 s; detection at 200 nm.* Dynamic coating was obtained by supplementing the BGE with 0.015 % (w/v) HPMC.

Symbols: (1) cytochrome *c*; (2) lysozyme; (3) trypsinogen; (4) chymotrypsinogen A

Table 4.1. Repeatability of migration time (tm, min.)[1] and corrected peak area (Area/tm)[1] of the studied standard basic proteins (25 μg/mL) under the optimised electrophoretic conditions[2].

cytochrome *c*		lysozyme		trypsinogen		chimotrypsinogen A	
tm	Area/tm	tm	Area/tm	tm	Area/tm	tm	Area/tm
6.89 (0.12)	2.049 (3.65)	7.62 (0.10)	4.33 (4.65)	9.25 (0.15)	4.58 (4.50)	9.63 (0.20)	3.417 (4.0)

[1] Mean values and (RSD %) for n = 3.

[2] CE conditions as in Fig. 4.3 (a).

3.2. Analytical study of the acetylated histone H4 isoforms. Effect of histone deacetylase inhibitors

The treatment of cells with HDAC inhibitors results in the increase of highly acetylated forms of histones, which affect gene expression, cell differentiation, and apoptosis. Recently, LC-MS was used for the first time in monitoring the variations in the acetylation and methylation state of the core histones after HDACs inhibitors treatment in a human colon cancer cell line (HT29) [11]. In the present study, identification and quantitation of H4 acetylated isoforms was carried out by means of different integrated techniques: LC-MS, MALDI-TOF MS and CE on pullulan-coated capillary.

3.2.1. HPLC-MS analysis

As the first step of our investigation, a LC-UV-ESI-ion trap MS analysis of the mixture of core histones (control) was performed; The peaks were identified by deconvoluted ESI mass spectra and their identity has been reported as it appears in the figure 4.2. A peak eluting at 49 min. was identified as histone H4 (Fig. 4.4) as result by the deconvoluted ESI mass spectra achieved by an on-line ion trap with Mag Tran 1.0 software (Fig. 4.5). Each protein modification was indicated by the derived molecular mass calculated by the software, as reported in Table 4.2 along with their relative percentage. These results revealed the presence of approximately 60 % of monoacetylated (including the mono- and dimethylated) forms, 36 % of the diacetylated (including the mono- and dimethylated) forms and 4 % of the triacetylated (including mono-, di- and trimethylated) forms.

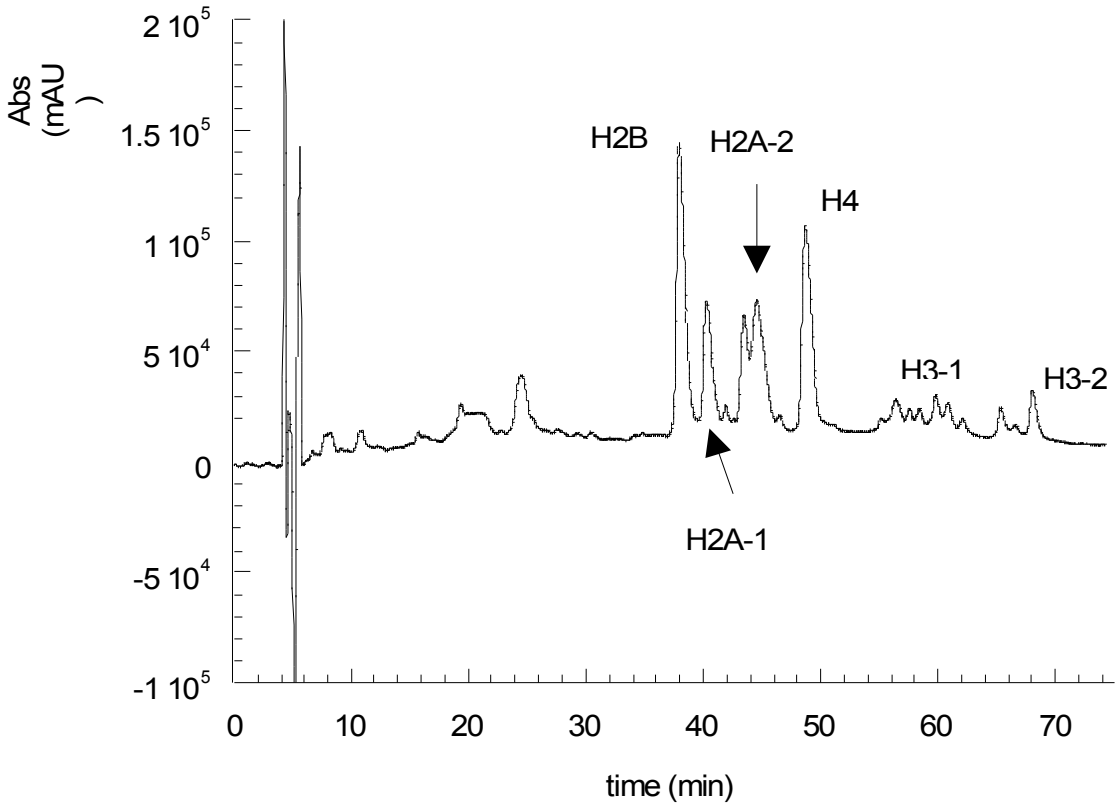

Fig. 4.4. Reversed-phase LC-UV chromatogram of the studied core histones (control sample). Conditions as in the text.

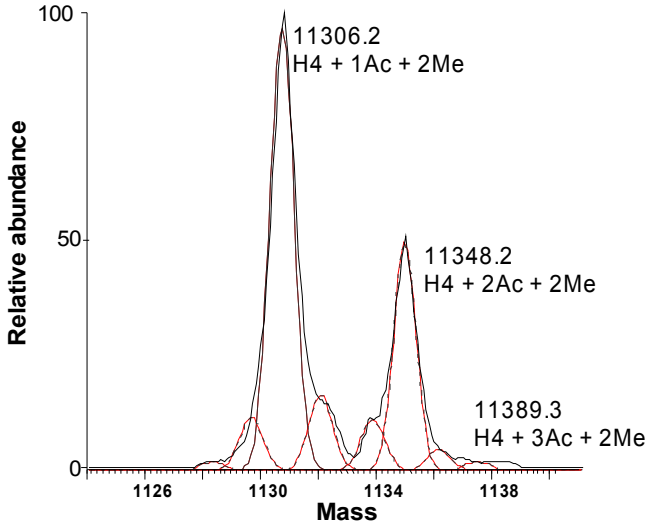

Fig. 4.5. MALDI-time of flight spectrum of histone H4 digested by arginase. MS analysis of Arg-C digest of his tone H4 isolated by RP-LC from histone extract of control cells. The signals at m/z 1612.9612, 1654.9456 and 1696.9324 correspond to the molecular masses of peptide 1-17 mono, di and tri-acetylated. The signals at m/z 1906.0114, 1949.0049and 1991.0010 correspond to the molecular masses of peptide 1-19 mono, di and tri-acetylated. The signals at m/z 2143.2221, 2300.1450, 2347.1981 and 2504.0112 correspond to peptides di-methylated at K20.

Table 4.2. Distribution of histone H4 isoforms in control samples

Derived mass (Da) ± SD	Interpretation	Found % ± SD
11279.2 ± 0.1	H4 + 1 Acet	2.84 ± 1.93
11292.8 ± 0.9	H4 + 1 Acet + 1 Met	5.38 ± 0.88
11306.2 ± 1.5	H4 + 1 Acet + 2 Met	52.43 ± 0.98
11320.9 ± 0.8	H4 + 2 Acet	9.90 ± 0.81
11335.1 ± 1.0	H4 + 2 Acet + 1 Met	4.77 ± 1.87
11348.2 ± 1.4	H4 + 2 Acet + 2 Met	21.77 ± 0.50
11362.4 ± 1.1	H4 + 3 Acet	2.91 ± 0.60
11376.6 ± 1.6	H4 + 3 Acet + 1 Met	0.70 ± 1.02
11390.4 ± 0.8	H4 + 3 Acet + 2 Met	0.00 ± 0.00
11405.1 ± 1.4	H4 + 4 Acet	0.00 ± 0.00

Derived masses and quantitative results are the mean of three indipendent histone extractions and subsequent LC-ESI-IT MS analysis and are expressed as modified form percentage with histone H4. Ac, acetylation (+42); Me, methylation (+14).

In order to determine the sites of acetylation, *i.e.* the specific lysin residues involved in the post-translational H4 histone modifications, we carried out digestion with endoproteinase Arg-C, a selective enzyme which cleaves proteins in the arginine sites [20], followed by MALDI-TOF MS analysis. Hence, H4 histone isolated by RP-LC from the histone extract of control cells was incubated with endoproteinase Arg-C overnight and subjected to the mass analysis. The Arg-C digest spectrum obtained by MALDI-TOF is reported in Fig. 4.6.

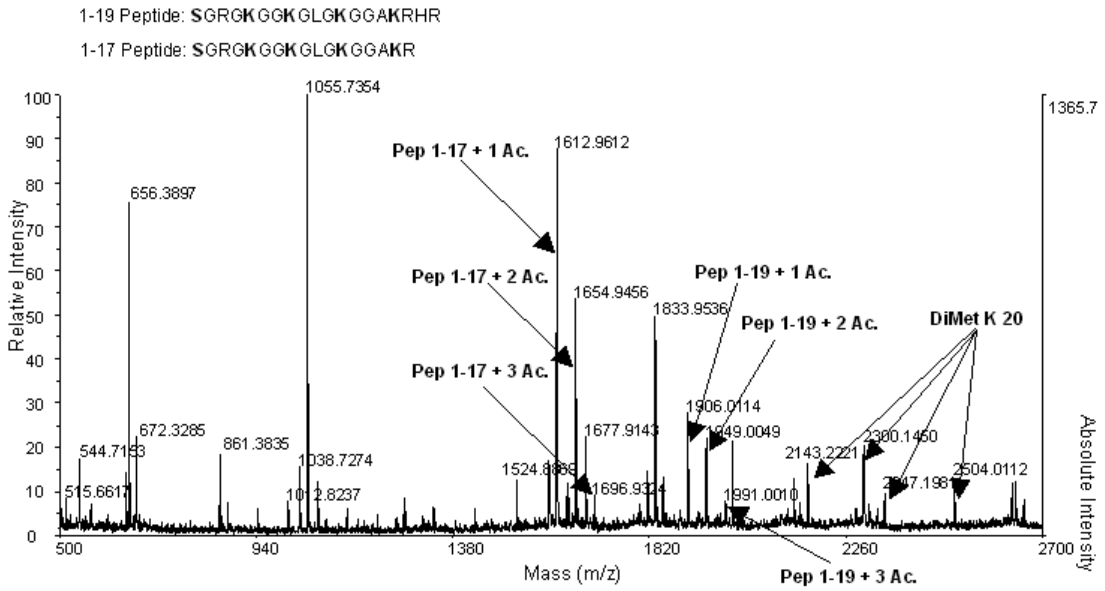

Fig. 4.6. MALDI-time of flight spectrum of histone H4 digested by arginase. MS analysis of Arg-C digest of his tone H4 isolated by RP-LC from histone extract of control cells. The signals at m/z 1612.9612, 1654.9456 and 1696.9324 correspond to the molecular masses of peptide 1-17 mono, di and tri-acetylated. The signals at m/z 1906.0114, 1949.0049and 1991.0010 correspond to the molecular masses of peptide 1-19 mono, di and tri-acetylated. The signals at m/z 2143.2221, 2300.1450, 2347.1981 and 2504.0112 correspond to peptides di-methylated at K20.

The signals at m/z 1,612.9612, 1,654.9456 and 1,696.9324 were assigned to the molecular masses of peptide 1-17 mono- di- and tri-acetylated respectively. The signals at m/z 1,906.0114, 1,949.0049 and 1,991.0010 were attributed to the molecular masses of peptide 1-19 mono-, di- and tri-acetylated respectively, whereas the signals at m/z 2,143.2221, 2,300.1450, 2,347.1981 and 2,504.0112 were assigned to peptides di-methylated at K20 respectively.

The results of the MALDI-TOF MS study demonstrated that acetylation as a post-translational modification occurs in the H4 histone tail (Aminoacid sequence 1-20). The relative intensity of the peptide signals was found in agreement with the relative abundance of the intact H4 isoforms mono-, di- and tri-acetylated in control cells (Table 4.3). Moreover, the abundance of dimethylated isoforms was confirmed by the abundance of signals containing dimethylation at K20.

Table 4.3. Data of MALDI-TOF analysis on histone H4 after Arg-C digestion

Peptide	Number of Acetylation	Relative abundance
1-19 (SGRGKGGKGLGKGGAKRHR)	**1**	**51.7 ± 3.02**
	2	**38.92 ± 1.94**
	3	**9.38 ± 4.96**
1-17 (SGRGKGGKGLGKGGAKR)	**1**	**59.72 ± 1.85**
	2	**35.63 ± 1.87**
	3	**4.63 ± 0.03**

3.2.2. CE analysis

The interest in characterization of histones by CE prompted us to determine whether the system based on pullulan-coated capillary can be directly applied in the rapid separation of differently acetylated histones isoforms using standard BGEs without addition of any dynamic coating. In this regard, real samples corresponding to the histones fractions, as identified by LC-ESI-MS, were collected after repeated HPLC-UV runs and used for CZE analysis. Under the previously optimized CE conditions (100 mM Tris-phosphate, pH 2.5, BGE, in a pullulan-coated capillary) the analysis allowed multiple peaks to be separated, thus indicating an improved selectivity and resolution compared to the HPLC approach. (Fig. 4.7)

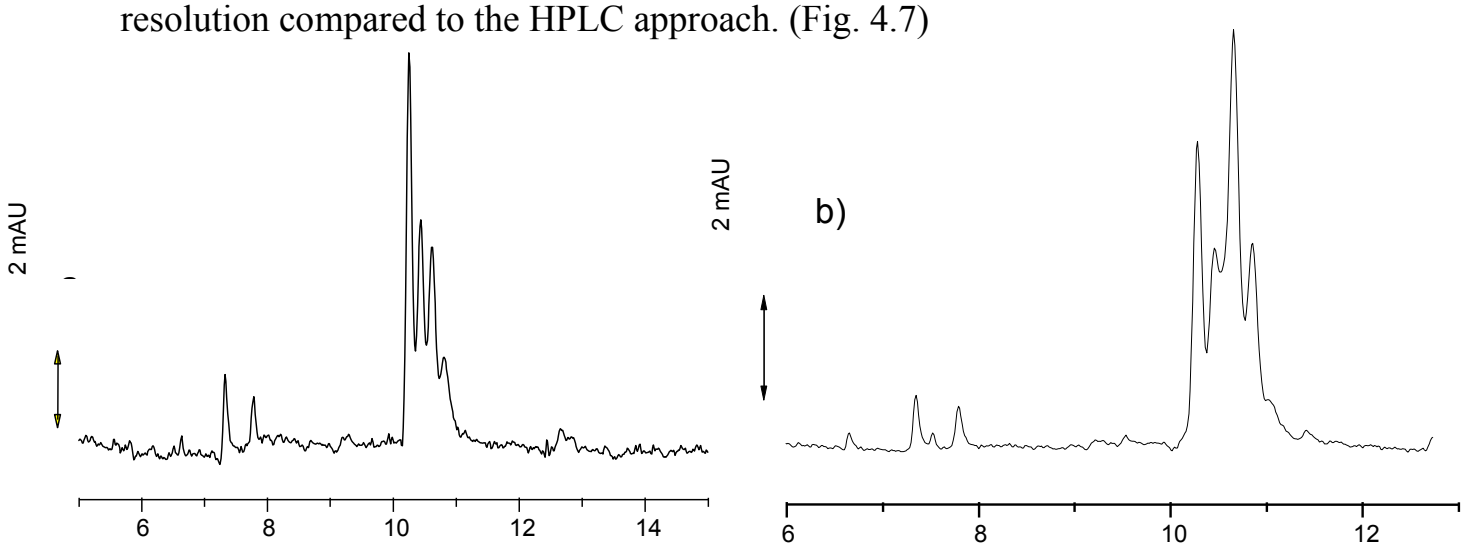

Fig. 4.7. Electropherograms of single histones fractions: a)H1-1 and b) H1-2. CE conditions: pullulan-coated capillary of 48.5 cm total length (40 cm effective length; i.d. 50 mm); BGE: pH 2.5 Tris-phosphate (100 mM); voltage at 15 kV; temperature at 30 °C; hydrodynamic injection at 50 mbar x 3 s; detection at 200 nm.

Our interest was however direted to histone H4 due to its high level of acetylated

isoforms. Using the conventional buffer the separation was not satisfactory due to band broadening. By a simple change of the counter ion nature of BGE, triethanolamine instead of Tris-base, a noticeable improvement of separation and peak shape was achieved. In Fig. 4.8 the electropherograms of histone H4 samples, purified by HPLC from HT29 cell line, are reported. In particular, in Fig. 4.8a the CE resolution of histone H4 obtained from an untreated HT29 (control sample) is reported; as it can be seen, two sharp-cut peaks were baseline separated and a third one lower was evident. Since the separation under the applied conditions is driven by zonal electrophoresis, the migration order of the peaks should be related to the charge-to-mass ratio. The acetylation of H4 histone results in a decrease of the overall positive charge of the protein caused by the loss in basicity of the acetylated nitrogen; this will result in diminish the electrophoretic mobility. As a consequence, the monoacetylated, diacetylated and triacetylated variants of H4 histone should migrate in the reported order. On the other hand, it can be reasonably assumed that the methylation of nitrogen does not affect the overall charge of the histones and a merely slight increase of molecular mass should be observed in comparison to the acetylated forms. However the increase of molecular mass due to the nitrogen methylation could hardly differentiate the mobility of such heavy molecules. Therefore it seemed to be acceptable that each of the peaks obtained in CE separation is a mixture of differently methylated forms of a determinate acetylated histone.

This observation was found to be consistent with the LC-ESI-ion trap MS quantitative data on the relative percentages of each acetylated form (Table 4.2) and was further confirmed by the variation of the CE peak area response in the analysis of the differently treated samples.

In particular, in Fig. 4.8b and Fig. 4.8c, the electropherograms of histone H4 from HT29 treated with sodium butyrate and 9-HSA, respectively, are reported. Butyrate was previously tested on human leukaemia and various cancer cell lines [21, 22], and, in our laboratory, on HT29 cell line [11]. Its use resulted in a histone hyperacetylation, which eventually caused apoptosis; the increase in the relative

proportion of highly acetylated forms was correlated with the inhibition of HDACs enzymatic activity. The treatment with butyrate induced the decreasing of the monoacetyl- H4 (44.2% ± 0.85), whereas diacetyl- H4 content (47.3% ± 0.66) and the triacetyl forms (8.5% ± 0.95) increased significantly (Fig. 4.8b). On the other hand, 9-hydroxystearic acid (9-HSA) an endogenous lipid peroxidation by-product that greatly diminishes in tumors, causing as a consequence the loss of one of the control mechanisms on cell division, was previously shown to control cell growth and differentiation by inhibiting HDAC activity in vitro [23]. In this regard, analysis of HT29 histones after treatment with a physiologically relevant concentration of 9-HSA (100 μM) produced a slight increase of acetylated H4 isoforms (Fig. 4.8c).

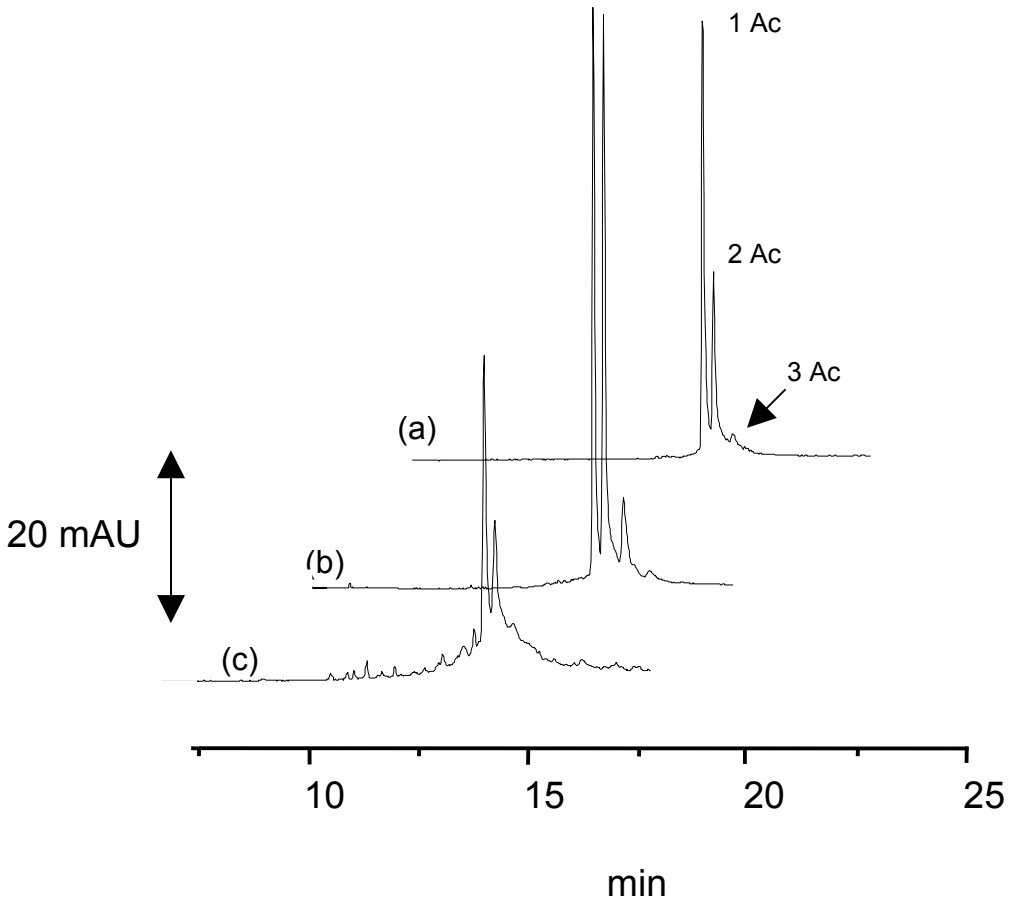

Fig. 4.8. Electropherograms of H4 histone in different samples. (a) control sample (untreated); (b) treated with sodium butyrate and (c) treated with 9-HSA.

CE conditions: pullulan-coated capillary of 48.5 cm total length (40 cm effective length; i.d. 50 mm); BGE constituted of a pH 2.5 triethanolamine-phosphate (100 mM); voltage at 10 kV; temperature at 40 °C; hydrodynamic injection at 50 mbar x 3 s; detection at 200 nm.

Symbols: 1 Ac; 2 Ac and 3 Ac corresponded to the differently acetylated isoforms of histone H4.

4. Conclusion

Pullulan-coated capillaries showed to be useful in CZE of basic proteins showing excellent repeatability of migration time and peak area. In particular, this capillary coating was successful in the CZE analysis of histone H4 acetylated isoforms. The obtained results were interesting because of the rapidity and selectivity of separation, also in comparison with the previous CE approaches based on the use of additives to the BGE. The proposed method allowed the percentage quantitation of acetylated (monoacetylated, diacetylated and triacetylated) isoforms of histone H4 with the aim to monitor its acetylation level in cell lines treated with different HDAC inhibitors. Although the results need for further studies on a higher number of samples and, if necessary, minor arrangements in view of CE-MS hyphenation, it can be concluded that the proposed method can offer an important complementary support to the HPLC-MS analysis of these complex biological samples.

References

[1] C.B. Wilson, M. Merkenschlager, Curr. Opin. Immunol. 18 (2006) 143.

[2] M. Jung, Curr. Med. Chem. 8 (2001) 1505.

[3] R.W. Johnstone, Nat. Rev. Drug Discov. 1 (2002) 287.

[4] P.A. Marks, V.M. Richon, R. Breslow, R.A. Rifkind, Curr. Opin. Oncol. 13 (2001) 477.

[5] H. Lindner, W. Helliger (1997) Capillary electrophoresis in Biotechnology and Environmental Analysis. In: Parvez P, Caudy S, Parvez P, Roland-Gosselin P (eds) Progress in HPLC-CE Series Vol 5. VSP, Utrecht

[6] H. Lindner, W. Helliger, A. Dirschlmayer, M. Jaquemar, B. Puschendorf, Biochem. J. 283 (1992) 467.

[7] M.F. Fraga, E. Ballestar, A. Villar-Garea, M. Boix-Chornet, J. Espada, G. Scotta, T. Bonaldi, C. Haydon, S. Ropero, K. Petrie, N.G. Iyer, A. Perez-Rosado, E. Calvo, J.A. Lopez, A. Cano, M.J. Calasanz, D. Colomer, M.A. Piris, N. Ahn, A. Imhof, C. Caldas, T. Jenuwein, M. Esteller, Nature genetics 37 (2005) 391.

[8] M. Boix-Chornet, M.F. Fraga, A. Villar-Garea, R. Caballero, J. Espada, A. Nunez, J. Casado, C. Largo, J.I. Casal, J.C. Cigudosa, L. Franco, M. Esteller, E. Ballestar, J. Biol. Chem. 281 (2006) 13540.

[9] R. Gotti, E. Calleri, G. Massolini, S. Furlanetto, V. Cavrini, Electrophoresis 27 (2006) 4746.

[10] S.Olmo, R.Gotti, M.Naldi, V.Andrisano, N.Calonghi, C.Parolin, L.Masotti, V.Cavrini, Anal. And Bioanal. Chem. doi: 10.1007/s00216-008-1903-5

[11] M. Naldi, V. Andrisano, J. Fiori, N. Calonghi, E. Pagnotta, C. Parolin, G. Pieraccini, L. Masotti, J. Chromatogr. A 1129 (2006) 73.

[12] I. Rodriguez, S.F.Y. Li, Anal. Chim. Acta 383 (1999) 1.

[13] J. Horvath, V. Dolnik, Electrophoresis 22 (2001) 644.

[14] V. Dolnik, Electrophoresis 27 (2006) 126.

[15] V. Dolnik, Electrophoresis 28 (2007) DOI 10.1002/elps.200700584

[16] R. Haselberg, G.J. de Jong, G.W. Somsen, J. Chromatogr. A 1159 (2007) 81.

[17] X. Fu, L. Huang, F. Gao, W. Li, N. Pang, M. Zhai, H. Liu, M. Wu, Electrophoresis 28 (2007)1958.

[18] J-L. Liao, J. Abramson, S. Hjertèn, J. Cap. Elec. 2 (1995) 191.

[19] C. Aguilar, A.J.P. Hofte, U.R. Tjaden, J. Van der Greef, J. Chromatogr. A 926 (2001) 57.

[20] E. McKittrick, P.R. Gafken, K. Ahmad, S. Henikoff, PNAS 101 (2004) 1525.

[21] J.R. Davie, J. Nutr. 133 (2003) 2485.

[22] G. Iacomino, M.C. Medici, D. Napoli, G.L. Russo, J. Cell. Biochem. 99 (2006) 1122.

[23] N. Calonghi, C. Cappadone, E. Pagnotta, C. Boga, C. Bertucci, J. Fiori, G. Tasco, R. Casadio, L. Masotti, J. Lipid. Res. 46 (2005) 1596.